Range-wide variation in local adaptation and phenotypic plasticity of fitness-related traits in Fagus sylvatica and their implications under climate change

Garate-Escamilla, Homero

2019-09

Garate-Escamilla , H , Hampe , A , Vizcaino-Palomar , N , Robson , T M & Garzon , M B 2019 , ' Range-wide variation in local adaptation and phenotypic plasticity of fitness-related traits in Fagus sylvatica and their implications under climate change ' , Global Ecology and Biogeography , vol. 28 , no. 9 , pp. 1336-1350 . https://doi.org/10.1111/geb.12936 , https://doi.org/10.1101/513515

http://hdl.handle.net/10138/310907
https://doi.org/10.1111/geb.12936

unspecified
submittedVersion

Global Ecology and Biogeography

A
Mac

Range-wide variation in local adaptation and phenotypic plasticity of fitness-related traits in Fagus sylvatica and their implications under climate change

Journal:	*Global Ecology and Biogeography*
Manuscript ID	GEB-2018-0597.R2
Manuscript Type:	Research Papers
Keywords:	phenotypic variation, species distribution models, beech, acclimation, trait co-variation, common gardens

Range-wide variation in local adaptation and phenotypic plasticity of fitness-related traits in *Fagus sylvatica* and their implications under climate change

Running title: range-wide multi-trait variation

Keywords: phenotypic variation, species distribution models, beech, acclimation, trait co-variation, common gardens

ABSTRACT

Aim: To better understand and more realistically predict future species distribution ranges, it is critical to account for local adaptation and phenotypic plasticity in populations' responses to climate. This is challenging because local adaptation and phenotypic plasticity are trait-dependent and traits co-vary along climatic gradients, with differential consequences for fitness. Our aim is to quantify local adaptation and phenotypic plasticity of vertical and radial growth, leaf flushing and survival across *Fagus sylvatica* range and to estimate each trait contribution to explain the species occurrence**.**

Location: Europe

Time period: 1995 – 2014; 2070

Major taxa studied: *Fagus sylvatica L.*

Methods: We used vertical and radial growth, flushing phenology and mortality of *Fagus sylvatica* L. recorded in BeechCOSTe52 (>150,000 trees). Firstly, we performed linear mixed-effect models that related trait variation and co-variation to local adaptation (related to the planted populations' climatic origin) and phenotypic plasticity (accounting for the climate of the

plantation), and we made spatial predictions under current and RCP 8.5 climates. Secondly, we combined spatial trait predictions in a linear model to explain the occurrence of the species.

Results: The contribution of plasticity to intra-specific trait variation is always higher than that of local adaptation, suggesting that the species is less sensitive to climate change than expected; different traits constrain beech's distribution in different parts of its range: the northernmost edge is mainly delimited by flushing phenology (mostly driven by photoperiod and temperature), the southern edge by mortality (mainly driven by intolerance to drought), and the eastern edge is characterised by decreasing radial growth (mainly shaped by precipitation-related variables in our model); considering trait co-variation improved single-trait predictions.

Main conclusions: Population responses to climate across large geographical gradients are dependent on trait x environment interactions, indicating that each trait responds differently depending on the local environment.

1. INTRODUCTION

Climate change is having a major impact on the structure, composition and distribution of forests worldwide (Trumbore *et al.*, 2015). Accordingly, numerous models have projected significant range shifts of forest tree species towards higher latitudes and elevations (Urban *et al.*, 2016). However, to date, the two most important processes in the response of tree populations to a rapidly changing climate, local adaptation and phenotypic plasticity (Savolainen *et al.*, 2007; Aitken *et al.*, 2008), are not systematically considered by species distribution models (Valladares *et al.*, 2014; Duputié *et al.*, 2015; Richardson *et al.*, 2017). Phenotypic plasticity enables a given genotype to express different phenotypes in response to changing environments, while local adaptation produces new genotypes with a greater ability to cope with the new environment. The two mechanisms are ubiquitous in natural populations, although their respective importance is considered to vary extensively through time and across species ranges (Reich *et al.*, 2016; Des Roches *et al.*, 2018). To persist under rapid climatic change, organisms with short generation times can take advantage of evolutionary responses and phenotypic plasticity (Scheepens *et al.*, 2018), whereas organisms with long generation cycles will rely predominantely on phenotypic plasticity (Fox *et al.*, 2019). To better understand and more realistically predict future species distribution ranges, it is therefore critical to identify and quantify the respective importance of local adaptation and phenotypic plasticity in the response of local populations to a changing climate.

From an ecological perspective, fitness can be associated with several phenotypic traits which directly affect survival and reproduction, creating a fitness landscape (Laughlin, 2018) that allows them to be used to bound species ranges (Benito-Garzón *et al.*, 2013; Stahl *et al.*, 2014). From a biogeographical perspective, higher fitness can be associated with higher probabilities of occurrence of a species in a given environment (Jiménez *et al.*, 2019). Fitness-related traits vary

across large geographical gradients, mainly depending on how natural selection drove differences among populations in the past. For instance, tree height is generally greatest at the core of a species range and decreases towards its margins (Purves, 2009; Pedlar & McKenney, 2017). Climate-driven mortality commonly increases towards the driest part of a species range, which is related to drought-induced stress conditions (Benito Garzón *et al.*, 2018). The onset of flushing phenology tends to be delayed towards high latitudes (Duputié *et al.*, 2015) as a consequence of genetic adaptation to late frost and fluctuating photoperiod (Way & Montgomery, 2015). Moreover, traits tend to co-vary across climatic gradients (Laughlin & Messier, 2015). A conspicuous example is the demographic compensation found between survival and growth near range margins (Doak & Morris, 2010; Benito-Garzón *et al.*, 2013; Peterson *et al.*, 2018), and further delimitation of species ranges based on demographic approaches (Merow *et al.*, 2017). New climatic conditions can result in maladaptation of some populations, which may change intra-specific patterns of trait variation and co-variation across geographical gradients, and eventually, species ranges. For example, increasing temperatures at high-latitude or high-elevation range margins are likely to produce higher growth rates, but they can also induce higher mortality owing to late frosts (Vitasse *et al.*, 2014; Delpierre *et al.*, 2017). Hence, species ranges are likely to be delimited by the interaction of multiple traits and their responses across environmental gradients (Benito-Garzón *et al.*, 2013; Stahl *et al.*, 2014; Enquist *et al.*, 2015).

Common gardens or provenance tests provide us with the necessary experiments to quantify phenotypic plasticity and local adaptation of fitness-related traits in response to climate (Mátyás, 1999). Models based on reaction norms of phenotypic traits using measurements recorded in common gardens show that: (i) geographic variation in populations' responses to climate is more strongly based on phenotypic plasticity than on local adaptation (Benito Garzón *et*

al., 2019); (ii) phenotypic variation can strongly differ among traits, in particular for survival of young trees, growth, and flushing phenology - traits that are directly related to fitness and typically measured in common gardens (Benito Garzón *et al.*, 2011; Valladares *et al.*, 2014; Duputié *et al.*, 2015; Richardson *et al.*, 2017); (iii) as a consequence, predictions of future species ranges are likely to be strongly influenced by the combined response of different fitness-related traits to climate (Laughlin, 2018), but this structured combination of intra-specific multi-trait variation defining species ranges has not been explored with empirical data.

Fagus sylvatica L. (European beech, henceforth "beech") is a widely distributed deciduous broadleaf temperate tree. In some parts of its range, beech has a late flushing strategy to avoid late frosts, which has a generally detrimental effect on tree growth (Gömöry & Paule, 2011; Robson *et al.*, 2013; Delpierre *et al.*, 2017). Beech is currently expanding at its northern distribution edge, whereas it experiences drought-induced radial growth decline and increasing mortality at its southern edge (Farahat & Linderholm, 2018; Stojnic *et al.*, 2018). The extent to which this pattern will continue in the future depends on how the combination of several fitness-related traits will influence the species' response to new climates.

Here, we propose a new modeling approach that quantifies local adaptation and phenotypic plasticity of four major phenotypic traits related to fitness (vertical and radial growth, young tree survival, and flushing phenology) and their interactions, to delimit species ranges under current and future climates. The four traits studied are expected to be under natural selection and show high heritability (Etterson, 2002; Delpierre *et al.*, 2017). Radial and vertical growth are directly related with biomass and thus reproduction (Younginger *et al.*, 2017), and the timing of flushing can affect fitness through reproduction success and growth by delimiting the growth season (Chuine, 2010). We use the phenotypic measurements recorded in the BeechCOSTe52 database

(Robson *et al.*, 2018), the largest network of common gardens for forest trees in Europe, covering virtually the entire distribution range of the species. Our specific objectives are: (i) to quantify range-wide patterns of phenotypic plasticity and local adaptation in growth, young tree survival and flushing phenology; (ii) to identify interactions among the different traits and the extent of their geographical variation in local adaptation and phenotypic plasticity; (iii) to discuss how these fitness-related traits delimit species ranges, and (iv) to better understand species ranges under new climate scenarios and the role of trait variation in shaping the future species range.

2. MATERIAL AND METHODS

We calibrated two types of linear mixed-effect models using a combination of trait measurements from common gardens where seeds coming from provenances from different origins have been planted (provenances) and of environmental variables that we obtained for these common gardens and provenances. The first model type (one-trait models) used single traits as response variables and environmental data as explanatory variables. The second model type (two-trait models) added a second trait as co-variate, which allowed the interaction of both traits to be accounted for in the model. Finally, to quantitatively estimate the contribution of each trait to explain beech range, we performed a binomial model using the occurrence of the species as response variable (presence/absence) and the spatial predictions of all traits as explanatory variables.

2.1. Trait measurements

We analyzed total tree height (vertical growth), diameter at breast height (DBH; radial growth), young tree survival and flushing phenology measured on a total of 153,711 individual beech trees

that originated from seeds collected from 205 populations (hereafter referred to as "provenances") across Europe and planted at 38 common gardens (hereafter "trials") (Figure 1). Briefly, the seeds were germinated in greenhouses and planted in the trials at an age of two years. Plantations were carried out in two consecutive campaigns, the first campaign (comprising 14 trials) in 1995 and the second one (comprising 24 trials) in 1998 (Robson *et al.*, 2018). This experimental design allowed us to attribute the effect of the climate at the trials to phenotypic plasticity and the effect of the climate at the provenance origin to genetics, including both the genetic structure and adaptive potential of the provenances. Young tree survival was recorded as individual tree survival. Leaf flushing was transformed from observational-stage score data (qualitative measurements that slightly differ among trials) to Julian days by adjusting flushing stages for each tree in every trial using the Weibull function (Robson *et al.*, 2011, 2013).

2.2. Environmental data

We used the EuMedClim database that gathers climatic information from 1901 to 2014 gridded at 1km (Fréjaville & Benito Garzón, 2018). The climate of the provenances was averaged for the period from 1901 to 1990, with the rationale that the seeds planted in the common gardens stemmed from trees growing during that period (Leites *et al.*, 2012). To characterize the climate of the common gardens, we calculated average values for the period between the date of planting (either 1995 or 1998) and the year of measurement of each trait for 21 climate variables (Supporting Information Table S1.2, Appendix S1).In addition, we used the latitude and longitude of the provenance and of the trial as proxies for the photoperiod and continentality, respectively (used in our flushing phenology models).

Phenotypic predictions under future climates were performed using the representative concentration pathway (RCP 8.5) in GISS-E2-R from WorldClim (http://www.worldclim.org/cmip5_30s) for 2070. We deliberately chose only this pessimistic scenario because for long-lived organisms such as forest trees it makes little difference whether the projected situation will be reached in 2070 or some decades later.

2.3. Statistical analysis

2.3.1. Spatial autocorrelation analysis

We performed a Moran's I analysis to check for spatial autocorrelation of vertical and radial growth, young tree survival, and leaf flushing. Correlograms were used to check autocorrelation variation with distance. We used the Moran.I function of the 'ape' package (Paradis *et al.*, 2018) and the 'Correlog' function of the 'pgirmess' package (Giraudoux *et al.*, 2018).

2.3.2. Environmental variable selection

To avoid co-linearity and reduce the number of environmental variables to use in models, we performed two principal component analyses (PCA), one for the climate variables related to the provenance site and one for the climate variables related to the trial site. For tree height, DBH and young tree survival, we considered 21 variables for the provenance and 21 variables for the trial (Supporting Information Figure S1.3, Appendix S1); whereas for leaf flushing, we only included the temperature-related variables as well as latitude and longitude (a total of 20 variables), because leaf flushing is known to be mainly driven by them (Basler & Körner, 2014).

The retained variables after the PCA screening were combined in models containing one variable to characterize the climate of the provenance and one variable to characterize the climate of the trial (Supporting Information Table S1.3, Appendix S1).

2.3.3. One-trait and two-trait mixed-effect models

We used linear mixed-effect models to analyze the response of individual traits (one-trait models) and the co-variation between two traits (two-trait models) to climate. We included the climate at the provenance and the trial site as previously selected (Supplementary Table 1), the age of trees, and for the leaf flushing model also latitude and longitude as fixed effects. The trial, blocks nested within the trial and trees nested within block and trial, were included as random effects to control for differences among sites and for repeated measurements of the same trees. The random effect of the provenance was also included in the model. The common form of the one-trait model was:

$$log(TR_{ijk}) = \alpha_0 + \alpha_1(Age_{ik}) + \alpha_2(CP_{ij}) + \alpha_3(CT_{ik}) + \alpha_4(CP_{ij}{}^2) + \alpha_5(CT_{ik}{}^2) + \alpha_6(Age_{ik} \times CP_{ij}) + \alpha_7 (Age_{ik} \times CT_{ik}) + \alpha_8(CP_{ij} \times CT_{ik}) + \beta + \varepsilon$$

(Equation 1)

Where TR = trait response of the i^{th} individual of the j^{th} provenance in the k^{th} trial; Age = tree age of the i^{th} individual in the k^{th} trial; CP = climate at the provenance site of the i^{th} individual of the j^{th} provenance; CT = climate at the trial site of the i^{th} individual in the k^{th} trial; β = random effects and ε = residuals. In addition, the model included the following interaction terms: Age and CP, Age and CT, and CP and CT.

We analyzed trait co-variation across the species range by adding two specific traits of interest in the same model. The common form of the two-trait model was:

$$log(TR_{ijk}) = \alpha_0 + \alpha_1(Age_{ik}) + \alpha_2(Cov_{ij}) + \alpha_3(CP_{ij}) + \alpha_4(CT_{ik}) + \alpha_5(Cov_{ik} \times CP_{ij}) + \alpha_6 (Cov_{ik} \times CT_{ik}) + \alpha_7(Cov_{ik} \times Age_{ik}) + \alpha_8(Age_{ik} \times CP_{ij}) + \alpha_9(Age_{ik} \times CT_{ik}) + \alpha_{10}(CP_{ij} \times CT_{ik}) + \beta + \varepsilon$$

(Equation 2)

Where TR = trait response of the i^{th} individual of the j^{th} provenance in the k^{th} trial; Age = tree age of the i^{th} individual in the k^{th} trial; Cov = trait co-variate of the i^{th} individual in the k^{th} trial; CP = climate at the provenance site of the i^{th} individual of the j^{th} provenance; CT = climate at the trial site of the i^{th} individual in the k^{th} trial; β = random effects and ε = residuals. In addition, the model included the following interaction terms: Cov and CP, Cov and CT, Cov and Age, Age and CP, Age and CT, and CP and CT.

The one-trait and two-trait models for vertical and radial growth and leaf flushing were fitted with the 'lmer' function, while the one-trait model for young tree survival was fitted with the 'glmer' function to accommodate logistic regressions (binomial family) in the analysis. We implemented a stepwise-model procedure with four main steps to choose the best supported model (Akaike, 1992): (i) we fitted saturated models that included all the variables in the fixed part of the model; (ii) we chose the optimal random component of the model by comparing the battery of models using restricted maximum likelihood (REML), and selected the best model using the Akaike information criterion (AIC) with criteria ΔAIC <2 (Mazerolle, 2006); (iii) we compared the battery of models using maximum likelihood (ML) and selected the optimal fixed component using the AIC criterion; (iv) we combined the best optimal random and fixed component

previously selected and adjusted them using REML to obtain the best performing model. All model fits were done using the package 'lme4' (Bates *et al.*, 2018).

For the best supported models, we visually analyzed the interactions of vertical growth, radial growth, young tree survival and leaf flushing with the environment (one-trait models) and between traits (between the response and co-variate variable, i.e. the two-trait models). To do so, tree age was fixed to 12 years for the radial and vertical growth and leaf flushing models and to 6 years for the young tree survival model. Mathematical interactions in one-trait models (CP x CT in equation 1) represent the differences in trait values that can be attributed to the provenance (interpretable as local adaptation) and those that can be attributed to the trial (interpretable as phenotypic plasticity). Mathematical interactions in two-trait models (Cov x CT in equation 2) represent the differences in trait values that can be attributed to a second trait that co-varies across the species range with the first trait, mediated by the climate of the trial (representing phenotypic plasticity). Unfortunately, young tree survival could not be included in the two-trait models because there were insufficient measurements shared with other traits in the same trials.

We estimated the percentage of the variance explained by the model attributed to the fixed effects alone (marginal R^2) and attributed to the fixed and random effects together (conditional R^2). We measured the generalization capacity (Pearson correlation) of the model using cross-validation (64% of the data used for calibration and the remaining 34% for validation).

2.3.4. Spatial predictions

We made spatial predictions for each trait across the species range for current and future climatic conditions using the 'raster' package (Hijmans *et al.*, 2017). For the prediction of current and future trait variation, the climate variable for provenance was represented by the average climate

over the period from 1901 to 1990. The climate of the trial was set as the average climate from 2000 to 2014, for current trait predictions, and to 2070 for future predictions. For two-trait models, the predicted values of the co-variate (DBH and leaf flushing) in the present were used to estimate the predictions of vertical growth in the future. We calculated the spatial difference between the future and the current conditions (future values minus current values) to illustrate the amount of change that traits can accommodate. All spatial predictions of traits were delimited within the distribution range of the species (EUFORGEN, 2009).

2.3.5. Quantification of the trait contribution to delimit the range of beech

Following the rationale that fitness-related, demographic and functional traits can shape species ranges (Stahl *et al.*, 2014; Merow *et al.*, 2017), we regressed the occurrence (presence/absence) of the species (EUFORGEN, 2009) against the trait values obtained by the one-trait models using the 'glm' function to accommodate logistic regressions (binomial family). The equation takes the form:

$$(RV) = \alpha_0 + \alpha_1(Vg) + \alpha_2(Rg) + \alpha_3(S) + \alpha_4(Lf) + \alpha_5(Vg \times S) + \alpha_6(Rg \times S) + \alpha_7(Lf \times S) + \alpha_8 (Vg \times Rg) + \alpha_9(Vg \times Lf) + \alpha_{10}(Rg \times Lf) + \varepsilon$$

(Equation 3)

Where RV = presence/absence of beech; Vg = vertical growth; Rg = radial growth; S = young tree survival; Lf = leaf flushing; ε = residuals. In addition, the model included all possible pairwise linear interactions of the included traits. The total deviance explained by the model was calculated using the function 'Dsquared' of the package 'modEvA' (Barbosa *et al.*, 2014). Then, we performed an analysis of variance (ANOVA) of the model to obtain trait and trait interaction deviances to estimate the percentage of the variance attributable to each trait.

All the models where performed with the R statistical framework version 3.2.0 (R Development Core Team, 2015).

3. RESULTS

3.1. Spatial autocorrelation analysis

Overall, the four studied traits were not significantly autocorrelated (Supporting Information Table S1.1, Appendix S1), although one autocorrelation point was found for young tree survival and leaf flushing using distance correlograms (Supporting Information Figure S1.1, Appendix S1).

3.2. Environmental variables selection

The two PCA performed (provenance PCA and trial PCA) revealed two groups of variables, one related with temperature and another more related with precipitation (Supporting Information Figure S1.2, Appendix S1). The two most important axes of the provenance PCA explained 53.52 and 24.03% of the total variance, and those of the trial PCA explained 38.93 and 24.19% (Supporting Information Figure S1.2, Appendix S1). To avoid co-linearity in the variables that we used in the model stepwise procedure, we retained the following variables for tree growth and young tree survival: BIO1, BIO5, BIO6, BIO12, BIO13, BIO14, PET Mean and PET Max. For the leaf flushing models, we retained BIO1, BIO5, BIO6, MTdjf, MTmam, MTjja, Mtson, and Mtdjfmam in addition to latitude and longitude.

3.3. One-trait and two-trait models

According to the best supported models (Table 1 and Supporting Information Table S1.3, Appendix S1), the most important variable related to the climate at the provenance for vertical growth, radial growth and young tree survival was maximal potential evapotranspiration (PET Max). The most important variables related to climate at the trials were precipitation of the wettest month (BIO13) for vertical growth, annual precipitation (BIO12) for radial growth, and precipitation of the driest month (BIO14) for young tree survival. In the case of leaf flushing, the mean temperature of December, January and February (MTdjf) was the most important climate variable for both the provenance and the trial site. The latitude of the provenance and the trial and the longitude of the trial were also significant in the leaf flushing model (see Supporting Information Table S1.3, Table S1.4, Appendix S1 for detailed statistics on the models). We observed significant interactions between the climate of the trial and that of the provenance in all models (Table 1; Supporting Information Table S1.4, Appendix S1).

The capacity for generalization from the models (Pearson correlation coefficients) was high: between 0.53 for radial growth and 0.73 for leaf flushing. The marginal R^2 ranged from 18% for the young tree survival model to 57% for the vertical growth model, while the conditional R^2 ranged from 40% for the young tree survival model to 98% for the radial growth model (Supporting Information Table S1.4, Appendix S1).

The significance of the fixed and random effects in the one-trait models was positively affected (i.e., estimates were higher) by the addition of a second trait (Supporting Information Table S1.5, Appendix S1). Furthermore, the co-variates and their interactions with the climate variables of the trials were also significant in the two-trait models (Supporting Information Table S1.5, Appendix S1). The capacity to generalize from the two-trait models was high: 0.76 for the vertical growth-radial growth model and 0.77 for the vertical growth-leaf flushing model

(Supporting Information Table S1.5, Appendix S1). The marginal R^2 was 62% in the vertical growth-radial growth model and 47% in the vertical growth-leaf flushing model, while the conditional R^2 was 95% in the vertical growth-radial growth model and 99% in the vertical growth-leaf flushing model (Supporting Information Table S1.5, Appendix S1).

3.4. Spatial patterns of phenotypic trait variation from one-trait models

Spatial predictions showed differences in phenotypic trait variation among traits (Figure 2, maps) and the interaction graphs permitted the way that plasticity and local adaptation shape these differences to be visualized (Figure 2, interaction graphs).

Vertical growth reached its maximum value at intermediate values of precipitation of the wettest month in the trials (Figure 2a, interaction graph). These largest trees were predicted to occur mostly over the northern and western part of the species range (Figure 2a, map). A signal of local adaptation to PET max was detected in our models and is shown by the interaction graph, where each line represents the response of provenances to high, intermediate and low levels of maximal potential evapotranspiration.

Predicted radial growth across the species range presented a similar pattern to that of vertical growth, but with the lowest values in marginal populations, particularly at the southern margin (Figure 21b, map). High annual precipitation coincided with high growth rates (Figure 2b map), with a moderate signal of local adaptation to PET max in the form of some variation among provenances (Figure 2b, interaction graph).

The lowest young tree survival rates were predicted towards the east and at some isolated points in the southernmost part of the range (Figure 2c, map). Young tree survival increased

towards those trials where precipitation is high in the driest month, with weak local adaptation to PET max indicated by very small –though statistically significant– differences among provenances (Figure 2c, interaction graph).

Earlier flushing was predicted towards the south-eastern part of the range (Fig 1d, map), with notable local adaptation indicated by large differences among provenances depending on the latitude of origin (Figure 2d, interaction graph). Differences in flushing date among provenances were particularly large in trials where the winter temperature is low (Figure 2d, interaction graph).

3.5. Patterns of phenotypic trait variation from two-trait models

Overall, models with a second trait as co-variate produced different results to those considering a single trait only. Predicted vertical growth was higher when either radial growth (Figure 3a) or leaf flushing (Figure 3b) was included as a co-variate than when no co-variates were considered (Figure 2a). Vertical growth increased with radial growth and precipitation (Figure 3a) and decreased in those regions where leaf flushing was predicted to be late in the year (which corresponded mainly to the northern part of the range) (Figure 3b).

3.6. Spatial predictions of traits under climate change considering one- and two-trait models

Trait projections for 2070 showed an overall increase in tree growth, particularly for radial growth (Figure 4a, b), but following similar spatial patterns to those predicted under current conditions (Figure 2a, b). Young tree survival was predicted to strongly decrease (with respect to that predicted under current conditions, Figure 2c) in the east and throughout the range periphery, while

young tree survival rates remained higher in the central part (Figure 4c). Leaf flushing showed similar patterns to those predicted under current conditions (Figure 2d) but with an overall advance in flushing dates (Figure 4d).

The prediction of vertical growth, considering radial growth as a covariate, showed an overall increase across the distribution range (Figure 4e) with respect to the model projection of vertical growth without radial growth as a covariate under future conditions (Figure 4a). Nevertheless, the predictions of vertical growth considering radial growth as a covariate (Figure 4e) showed an overall decrease in vertical growth, with some increases in vertical growth in the northern and northeastern range, compared to the same model applied to current conditions (Figure 3a; Supporting Information Figure S1.3e, Appendix S1). Predictions considering leaf flushing as a co-variate tended to constrain vertical growth throughout the range (Figure 4f) compared with the same model in current conditions (Figure 3b).

3.7. Total trait contribution to explain species ranges

All traits and their interactions significantly contributed to explain species occurrence (Table 2). The model explained 31% of the total deviance, with vertical growth accounting for 37%, radial growth for 33%, young tree survival for 19%, and leaf flushing for 1%. Please note that the different contribution of these four traits explaining species occurrence may be constrained by the nature of the data (particularly survival that is only measured in young trees). The interaction between vertical growth and young tree survival contributed with 3% to the total deviance, that between radial growth and leaf flushing with 2% and the remaining interactions with 1% or less (Table 2).

4. DISCUSSION

4.1. Contribution of phenotypic plasticity and local adaptation to range-wide variation in beech growth, young tree survival and leaf flushing

Altogether, our results underpin that range-wide variation in fitness-related traits of beech is driven markedly more by phenotypic plasticity than by local adaptation (Supporting Information Table S1.4, Appendix S1), as happens in other plant species (Benito Garzón *et al.*, 2019), and they imply that beech possesses a noteworthy capacity to respond to rapid climate change through acclimation. Although a short-term response through acclimation can be considered as positive for beech to keep pace with climate change, our results point out that the plastic component of tree growth and young tree survival is mostly related to precipitation (Table 1), which follows highly unpredictable patterns (Pflug *et al.*, 2018), making it difficult to evaluate whether acclimation will be enough for beeches to survive (our predictions for 2070 under RCP 8.5. showing an increase of mortality in young trees at the margins of the species ranges suggest that acclimation will not be great enough to permit the species to survive, at least at the margins of its range – Figure 4c). Local adaptation in tree growth (vertical and radial) and young tree survival are driven by adaptation to maximal potential evapotranspiration (Table 1), suggesting that populations are responding to selection factors related to drought (Volaire, 2018). This is in agreement with the general consensus that beech is a drought-sensitive species (Aranda *et al.*, 2015), although there is ongoing debate over the extent of resistance that beech has to drought (Pflug *et al.*, 2018).

The plastic response of leaf flushing to climate was mainly driven by winter temperatures (Table 1). There is a general consensus that winter temperatures will increase globally in the future (Vautard *et al.*, 2014), and, accordingly, our projection for 2070 anticipates an advance in flushing through most of the range (Figure 2d, 3d and S3d). However, leaf flushing can be constrained by local adaptation to photoperiod (Way & Montgomery, 2015; Gauzere *et al.*, 2017). The fact that phenotypic plasticity and local adaptation in leaf flushing are driven by different environmental parameters implies that these two processes would interact in the long-term. For instance, phenotypic plasticity concerning winter temperatures might enhance local adaptation towards new photoperiodical cues (i.e., shorter spring days), but the evolutionary time scale of local adaptation makes this interaction very unlikely in the short-term.

4.2 Trait relationships across the species range

Trait inter-dependence varied along geographical gradients as the two-trait models had higher predictive power and explained more variance than those based on a single trait (Supporting Information Table S1.4 and S1.5, Appendix S1). The tight albeit not perfect positive interaction between tree vertical and radial growth (Figure 3a, interaction graph) is unsurprising because of allometric relationships between these two variables, particularly in a common-garden plantation that avoids competition among trees.

The biological basis of the observed co-variation between vertical growth and leaf flushing is less obvious. One possible explanation is that vertical growth is greatly restricted by late flushing in northern beech populations (Kollas *et al.*, 2014). This would also explain our observation that the one-trait model predicts taller trees to occur in the North, whereas the two-trait model predicts

just the opposite. Interestingly, the two-trait model thus implies that strong local adaptation of leaf flushing to photoperiod tends to constrain phenotypic plasticity for vertical growth in northern beech populations (Way & Montgomery, 2015).

4.3. Are spatial patterns of growth, young tree survival and leaf flushing delimiting the range of beech?

Beech populations from certain eastern and southern parts of the distribution range seem most sensitive to climate, as suggested by the lowest values for all traits considered (Figure 2). In other parts of beech's range, different traits respond differently to climate, in line with the patterns found in annual plants and wood scrubs (Merow *et al.*, 2017). Our analysis of species occurrence as a function of spatial trait values also suggests that each of these traits and their interactions contributed to some extent to the delimitation of the species range (31% of the variance is explained by the four traits; Table 3). In particular: (i) young tree mortality delimits certain parts of the southern and eastern range of beech, reflecting the marginality due to climate continentality in these areas, and meaning that these populations are most threatened, thus making eastwards expansion of beech difficult (survival was exclusively measured in young trees, reflecting recruitment processes that are largely limited to climatically favorable years, indicating that more studies on regeneration and mortality are needed to confirm this result); this is the case for many species whose highest mortality is in the driest part of their range (Benito-Garzón *et al.*, 2013; Anderegg *et al.*, 2015; Camarero *et al.*, 2015); (ii) the smallest girths are predicted in the southern part of the distribution and the eastern part of the range, suggesting that radial growth is mostly restricted by drought (interaction graph and map, Figure 2b), as has already been pointed out (Farahat & Linderholm, 2018); (iii) with very little variation across climatic gradients, vertical

growth alone will not delimit beech range. This is not the case for other tree species, for which tree height is clearly delimiting species range (Chakraborty *et al.*, 2018), highlighting the fact that no single best trait delimits tree species ranges; (iv) projections of trees growing in southern and south-eastern regions that flush early also have higher mortality and lower growth predictions than elsewhere within the species range. However, when tree height and leaf flushing are pooled together in the two-trait model, this leads to an decrease in vertical growth in the North; (v) it seems that in beech, and likely in other species with local adaptation to photoperiod, phenology could restrict the northern expansion of ranges (Duputié *et al.*, 2015; Saltré *et al.*, 2015). Although the link between phenology, young tree survival and fitness is still unclear, and more experiments would provide a better understanding the interaction between photoperiod and phenology.

4.4. Implications of using trait approaches based on phenotypic variation to forecast beech sensitivity to climate change

Overall, spatial patterns of vertical and radial growth, young tree survival and leaf flushing predicted for the future (Figure 4), are relatively similar to those predicted by the models under current conditions (Figure 2 & 3). This might be due to the high plasticity of these traits that allows populations to respond to short-term changes in their environment, but other factors such as dispersal capacity, geographical or human barriers, and adjustment of climatic scenarios for the future would change our predictions. Our results, based on the study of phenotypic variation, predict species persistence in the future (if the occurrence of the species can be linked to high trait values (Merow *et al.*, 2017)) rather than extinction and migration northwards as predicted by species distribution models based on the occurrence of the species (Kramer *et al.*, 2010; Stojnic *et al.*, 2018).

Nevertheless, the direct comparison of our trait predictions for current and future conditions allows us to detect some differences in their spatial patterns and total trait values (Supporting Information Figure S1.3, Appendix S1), and gives us a better understanding of the temporal dynamics of traits and their relative importance for beech persistence in the future. For instance, our models of leaf flushing predict reduced geographical variability in phenology in the future (from day 94 to 160 -Figure 2d- and from day 94 to 147 – Figure 4d-), as has been reported worldwide (Ma *et al.*, 2018). This is mostly explained by larger advances in the phenology of populations at colder sites than those at warmer sites, likely as a consequence of the larger increases in winter temperatures that happen in the North (Kjellström *et al.*, 2018). Survival of young trees is predicted to decrease at the margins of the distribution, but less markedly than is predicted by species distribution models (Kramer *et al.*, 2010; Stojnic *et al.*, 2018). Although our spatial trait predictions do not perfectly match species occurrence, they explain the adaptive and plastic responses of populations' fitness-related traits to climate (Benito Garzón *et al.*, 2019).

Including more than one trait related to growth likely reflects a conserved allometric relationship between vertical and radial growth in the future (Figure 4e), but this may be a direct consequence of the lack of competition among trees in our experimental design. Including phenology in two-trait models seems to be detrimental for vertical growth, at least for northern populations where growth is likely constrained by phenology (Figure 4f). However, our trait co-variation approaches are limited to vertical growth as response variables, limiting our understanding of the interplay that other traits can have across species range in the future.

4.5. Limitations, perspectives and future research

Although this study relied on the largest network of common gardens for a forest tree in Europe, the resulting inferences suffer from a number of limitations. Our models are based on a limited set of ages (from 2 to 15 years old). However, the expression of phenotypic plasticity changes with age (Mitchell & Bakker, 2014), which can restrict the broad scope of our results to those ages that we considered. This limitation is particularly pronounced for the case of survival (age range 2 to 6 years), for which data only reflect early recruit survival. Our models of young tree mortality can also reflect the quality of the data from common gardens, where recruit survival was measured over a short study period and did not necessarily faithfully capture the regeneration potential of forest tree populations.

Tree growth and phenology are directly related to fitness (Chuine, 2010; Delpierre *et al.*, 2017; Younginger *et al.*, 2017). However, other relevant proxies for tree fitness as fecundity and reproduction have not been considered in our approach. In beech, climate warming tends to increase seed production in northern populations (Drobyshev *et al.*, 2010) and to cause a decline in seedling density in southern ones (Barbeta *et al.*, 2011), which would be expected to continue under climate change.

Our approach reflects the plastic and adaptive components of traits to determine their spatial distribution. Important elements of spatial ecology, such as geographical barriers and trees' dispersal capacity (Svenning & Skov, 2005), competition and other biotic interactions across large geographical gradients (Archambeau *et al.*, 2019) and those aspects related with the uncertainty of future climate (Nazarenko *et al.*, 2015), are not considered in our approach. . Adding these processes to our models would open a new perspective, to extend understanding of the realized niche of the species ranges. The genetic effect attributed to the provenances in our models includes both the genetic structure and the potential of populations to adapt. As more genomic information

on adaptive traits becomes available, models could incorporate the genomic basis of climate adaptation to help separate these different genetic effects (Bay *et al.*, 2018)

Our predictions should help to shape future controlled experiments on those populations most sensitive to climate (in the South – East of the range), and others designed to test those trait relationships that are still unclear (phenology – growth – mortality) at the northernmost distribution edge. Although both for beech, and for tree species in general, plasticity is thought to help populations to persist under climate change (Benito Garzon et al. 2019), evolutionary processes can play an crucial role for annual plants and those organisms with short generation cycles, permitting them to adapt to new climate conditions (Scheepens *et al.*, 2018; Fox *et al.*, 2019). Both theoretical and empirical studies on the interplay between phenotypic plasticity and local adaptation across organisms with different life-history strategies are needed to fully understand how these two processes modify populations' responses to climate change.

REFERENCES

Aitken, S.N., Yeaman, S., Holliday, J.A., Wang, T. & Curtis-Mclane, S. (2008) Adaptation , migration or extirpation : climate change outcomes for tree populations. *Evolutionary Applications*, 95–111.

Akaike, H. (1992) Data analysis by statistical models. *No To Hattatsu*, **24**, 127–133.

Anderegg, W.R.L., Flint, A., Huang, C., Flint, L., Berry, J.A., Davis, F.W., Sperry, J.S. & Field, C.B. (2015) Tree mortality predicted from drought-induced vascular damage. *Nature Geoscience*, **8**, 367–371.

Aranda, I., Cano, F.J., Gascó, A., Cochard, H., Nardini, A., Mancha, J.A., López, R. & Sánchez-Gómez,

D. (2015) Variation in photosynthetic performance and hydraulic architecture across European beech Fagus sylvatica L .) populations supports the case for local adaptation to water stress. *Tree Physiology*, **35**, 34–46.

Archambeau, J., Ruiz-Benito, P., Ratcliffe, S., Fréjaville, T., Changenet, A., Munoz Castaneda J., Lehtonen, A., Dahlgren, J., Zavala, M.A. & Benito Garzón, M. (2019) Similar patterns of background mortality across Europe are mostly driven by drought in European beech and a combination of drought and competition in Scots pine. https://www.biorxiv.org/content/10.1101/551820v1

Barbeta, A., Peñuelas, J., Ogaya, R. & Jump, A.S. (2011) Reduced tree health and seedling production in fragmented Fagus sylvatica forest patches in the Montseny Mountains (NE Spain). *Forest Ecology and Management*, **261**, 2029–2037.

Barbosa, A.M., Brown, J.A. & Real, R. (2014) modEvA – an R package for model evaluation and analysis. R package, version 0.1. Available at: http://modeva.r-forge.r-project.org/.

Basler, D. & Körner, C. (2014) Photoperiod and temperature responses of bud swelling and bud burst in four temperate forest tree species. *Tree Physiology*, **34**, 377–388.

Bates, D., Maechler, M., Bolker, B., Walker, S., Bojesen, R.H., Singmann, H., Dai, B., Scheipl, F., Grothendieck, G. & Green, P. (2018) lme4: Linear mixed-effects models using Eigen and S4. R package version 1.1-18-1. Available at: http://CRAN.R-project. org/package=lme4. *Available at: http://CRAN.R-project. org/package=lme4*.

Bay, R.A., Harrigan, R.J., Underwood, V. Le, Gibbs, H.L., Smith, T.B. & Ruegg, K. (2018) Genomic signals of selection predict climate-driven population declines in a migratory bird. *Science*, **359**, 83–86.

Benito-Garzón, M., Ruiz-Benito, P. & Zavala, M.A. (2013) Interspecific differences in tree growth and mortality responses to environmental drivers determine potential species distributional limits in

Iberian forests. *Global Ecology and Biogeography*, **22**, 1141–1151.

Benito Garzón, M., Alía, R., Robson, T.M. & Zavala, M.A. (2011) Intra-specific variability and plasticity influence potential tree species distributions under climate change. *Global Ecology and Biogeography*, **20**, 766–778.

Benito Garzón, M., Gonzalez Munoz, N., Wigneron, J.-P., Moisy, C., Fernandez-Manjarres, J. & Delzon, S. (2018) The legacy of water deficit on populations having experienced negative hydraulic safety margin. *Global Ecology & Biogeography*, **27**, 346–356.

Benito Garzón, M., Robson, T.M. & Hampe, A. (2019) ΔTraitSDM: species distribution models that account for local adaptation and phenotypic plasticity. *New Phytologist*. https://nph.onlinelibrary.wiley.com/doi/full/10.1111/nph.15716

Camarero, J.J., Gazol, A., Sancho-Benages, S. & Sangüesa-Barreda, G. (2015) Know your limits? Climate extremes impact the range of Scots pine in unexpected places. *Annals of Botany*, **116**, 917–927.

Chakraborty, D., Schueler, S., Lexer, M.J. & Wang, T. (2018) Genetic trials improve the transfer of Douglas-fir distribution models across continents. *Ecography*, **41**, 1–14.

Chuine, I. (2010) Why does phenology drive species distribution? *Philosophical Transactions of The Royal Society B Biological Sciences*, **365**, 3149–3160.

Delpierre, N., Guillemot, J., Dufrêne, E., Cecchini, S. & Nicolas, M. (2017) Tree phenological ranks repeat from year to year and correlate with growth in temperate deciduous forests. *Agricultural and Forest Meteorology*, **234–235**, 1–10.

Doak, D.F. & Morris, W.F. (2010) Demographic compensation and tipping points in climate-induced range shifts. *Nature*, **467**, 959–962.

Drobyshev, I., Övergaard, R., Saygin, I., Niklasson, M., Hickler, T., Karlsson, M. & Sykes, M.T. (2010) Masting behaviour and dendrochronology of European beech (Fagus sylvatica L.) in southern

Sweden. *Forest Ecology and Management*, **259**, 2160–2171.

Duputié, A., Rutschmann, A., Ronce, O. & Chuine, I. (2015) Phenological plasticity will not help all species adapt to climate change. *Global Change Biology*, **21**, 3062–3073.

Enquist, B.J., Norberg, J., Bonser, S.P., Violle, C., Webb, C.T., Henderson, A., Sloat, L.L. & Savage, V.M. (2015) Scaling from Traits to Ecosystems: Developing a General Trait Driver Theory via Integrating Trait-Based and Metabolic Scaling Theories. *Advances in Ecological Research*, **52**, 249–318.

Etterson, J.R. (2002) Constraint to Adaptive Evolution in Response to Global Warming. *Science*, **294**, 151–154.

EUFORGEN (2009) Distribution map of Beech (Fagus sylvatica). Available at: www.euforgen.org. *www.euforgen.org*, 1.

Farahat, E. & Linderholm, H.W. (2018) Growth–climate relationship of European beech at its northern distribution limit. *European Journal of Forest Research*, **137**, 1–11.

Fox, R.J., Donelson, J.M., Schunter, C., Ravasi, T. & Gaitán-Espitia, J.D. (2019) Beyond buying time: the role of plasticity in phenotypic adaptation to rapid environmental change. *Philosophical Transactions of the Royal Society B: Biological Sciences*, **374**, 20180174.

Fréjaville, T. & Benito Garzón, M. (2018) The EuMedClim Database: Yearly Climate Data (1901 – 2014) of 1 km Resolution Grids for Europe and the Mediterranean Basin. *Frontiers in Ecology and Evolution*, **6**, 1–5.

Gauzere, J., Delzon, S., Davi, H., Bonhomme, M., Garcia de Cortazar-Atauri, I. & Chuine, I. (2017) Integrating interactive effects of chilling and photoperiod in phenological process-based models. A case study with two European tree species: Fagus sylvatica and Quercus petraea. *Agricultural and Forest Meteorology*, **244–245**, 9–20.

Giraudoux, P., Antonietti, J.-P., Beale, C., Pleydell, D. & Treglia, M. (2018) Package 'pgirmess'.

Available at: https://cran.r-project.org/web/packages/pgirmess/pgirmess.pdf.

Gömöry, D. & Paule, L. (2011) Trade-off between height growth and spring flushing in common beech (*Fagus sylvatica* L.). *Annals of Forest Science*, **68**, 975–984.

Hijmans, R.J., Van Etten, J., Cheng, J., Mattiuzzi, M., Sumner, M., Greenberg, J.A., Perpinan Lamigueiro, O., Bevan, A., Racine, E.B., Shortridge, A. & Ghosh, A. (2017) Package 'raster': Geographic Data Analysis and Modeling. Available at: https://cran.r-project.org/web/packages/raster/raster.pdf.

Jiménez, L., Soberón, J., Christen, J.A. & Soto, D. (2019) On the problem of modeling a fundamental niche from occurrence data. *Ecological Modelling*, **397**, 74–83.

Kjellström, E., Nikulin, G., Strandberg, G., Christensen, O.B., Jacob, D., Keuler, K., Lenderink, G., van Meijgaard, E., Schär, C., Somot, S., Sørland, S.L., Teichmann, C. & Vautard, R. (2018) European climate change at global mean temperature increases of 1.5 and 2 degrees C above pre-industrial conditions as simulated by the EURO-CORDEX regional climate models. *Earth System Dynamics*, **9**, 459–478.

Kollas, C., Körner, C. & Randin, C.F. (2014) Spring frost and growing season length co-control the cold range limits of broad-leaved trees. *Journal of Biogeography*, **41**, 773–783.

Kramer, K., Degen, B., Buschbom, J., Hickler, T., Thuiller, W., Sykes, M.T. & de Winter, W. (2010) Modelling exploration of the future of European beech (Fagus sylvatica L.) under climate change-Range, abundance, genetic diversity and adaptive response. *Forest Ecology and Management*, **259**, 2213–2222.

Laughlin, D.C. (2018) Rugged fitness landscapes and Darwinian demons in trait-based ecology. *New Phytologist*, **217**, 501–503.

Laughlin, D.C. & Messier, J. (2015) Fitness of multidimensional phenotypes in dynamic adaptive landscapes. *Trends in Ecology & Evolution*, **30**, 487–496.

Leites, L.P., Robinson, A.P., Rehfeldt, G.E., Marshall, J.D. & Crookston, N.L. (2012) Height-growth response to changes in climate differ among populations of interior Douglas-fir: a novel analysis of provenance-test data. *Ecological Applications*, **22**, 154–165.

Ma, Q., Huang, J., Hänninen, H. & Berninger, F. (2018) Agricultural and Forest Meteorology Reduced geographical variability in spring phenology of temperate trees with recent warming. *Agricultural and Forest Meteorology*, **256–257**, 526–533.

Mátyás, C. (1999) Forest genetics and sustainability. *Dordrecht, Boston: Kluwer Academic Publishers*.

Mazerolle, M.J. (2006) Improving data analysis in herpetology: Using Akaike's information criterion (AIC) to assess the strength of biological hypotheses. *Amphibia Reptilia*, **27**, 169–180.

Merow, C., Bois, S.T., Allen, J.M., Xie, Y. & Silander, J.A. (2017) Climate change both facilitates and inhibits invasive plant ranges in New England. *Proceedings of the National Academy of Sciences*, **114**, E3276–E3284.

Mitchell, R.M. & Bakker, J.D. (2014) Intraspecific Trait Variation Driven by Plasticity and Ontogeny in Hypochaeris radicata. *PLoS ONE*, **9**.

Nazarenko, L., G. A. Schmidt, R. L. Miller, N. Tausnev, M. Kelley, R. Ruedy, G.L.R., I. Aleinov, M. Bauer, S. Bauer, R. Bleck, V. Canuto, Y. Cheng, T. L. Clune, a. D.D.G., G. Faluvegi, J. E. Hansen, R. J. Healy, N. Y. Kiang, D. Koch, A. A. Lacis, a. N.L., J. Lerner, K. K. Lo, S. Menon, V. Oinas, J. Perlwitz, M. J. Puma, D. Rind, a. R., M. Sato, D. T. Shindell, S. Sun, K. Tsigaridis, N. Unger, A. Voulgarakis, M.-S.Y. & Zhang, and J. (2015) Future climate change under RCP emission scenarios with GISS ModelE2. *Journal of Advances in Modeling Earth Systems*, 244–268.

Paradis, E., Blomberg, S., Bolker, B., Brown, J., Claude, J., Cuong, H.S., Desper, R., Didier, G., Durand, B., Dutheil, J., Ewing, R., Gascuel, O., Guillerme, T., Heibl, C., Ives, A., Jones, B., Krah, F., Lawson, D., Lefort, V., Legendre, P., Lemon, J., Marcon, E., McCloskey, R., Nylander, J., Opgen-Rhein, R., Popescu, A.-A., Royer-Carenzi, M., Schliep, K., Strimmer, K. & Vienne, D. de (2018)

Package 'ape' : Analyses of Phylogenetics and Evolution. Available at: https://cran.r-project.org/web/packages/ape/ape.pdf.

Pedlar, J.H. & McKenney, D.W. (2017) Assessing the anticipated growth response of northern conifer populations to a warming climate. *Scientific Reports*, **7**, 1–10.

Peterson, M.L., Doak, D.F. & Morris, W.F. (2018) Both life-history plasticity and local adaptation will shape range-wide responses to climate warming in the tundra plant Silene acaulis. *Global Change Biology*, **24**, 1614–1625.

Pflug, E.E., Buchmann, N., Siegwolf, R.T.W., Schaub, M., Rigling, A. & Arend, M. (2018) Resilient Leaf Physiological Response of European Beech (Fagus sylvatica L.) to Summer Drought and Drought Release. *Frontiers in Plant Science*, **9**, 187.

Purves, D.W. (2009) The demography of range boundaries versus range cores in eastern US tree species. *Proceedings of the Royal Society B: Biological Sciences*, **276**, 1477–1484.

R Development Core Team, R. (2015) R: A Language and Environment for Statistical Computing. R Foundation for Statistical Computing, Vienna, Austria. Avaliable at: http://www.Rproject. org.

Reich, P.B., Sendall, K.M., Stefanski, A., Wei, X., Rich, R.L. & Montgomery, R.A. (2016) Boreal and temperate trees show strong acclimation of respiration to warming. *Nature*, **531**, 633–636.

Richardson, B.A., Chaney, L., Shaw, N.L. & Still, S.M. (2017) Will phenotypic plasticity affecting flowering phenology keep pace with climate change? *Global Change Biology*, **23**, 2499–2508.

Robson, T.M., Alia, R., Bozic, G., Clark, J., Forsteuter, M., Gomory, D., Liesebach, M., Mertens, P., Rasztovits, E., Zitová, M. & von Wühlisch, G. (2011) The timing of leaf flush in European beech (Fagus sylvatica L.) saplings. *Genetic Resources of European Beech (Fagus sylvatica L.) for Sustainable Forestry: Proceedings of the COST E52 Final Meeting. SERIE FORESTAL*, **22**, 61–80.

Robson, T.M., Benito Garzón, M. & BeechCOSTe52 database consortium (2018) Data Descriptor: Phenotypic trait variation measured on European genetic trials of Fagus sylvatica L. *Scientific Data*,

5, 1–7.

Robson, T.M., Rasztovits, E., Aphalo, P.J., Alia, R. & Aranda, I. (2013) Flushing phenology and fitness of European beech (Fagus sylvatica L.) provenances from a trial in La Rioja, Spain, segregate according to their climate of origin. *Agricultural and Forest Meteorology*, **180**, 76–85.

Des Roches, S., Post, D.M., Turley, N.E., Bailey, J.K., Hendry, A.P., Kinnison, M.T., Schweitzer, J.A. & Palkovacs, E.P. (2018) The ecological importance of intraspecific variation. *Nature Ecology & Evolution*, **2**, 57–64.

Saltré, F., Duputié, A., Gaucherel, C. & Chuine, I. (2015) How climate, migration ability and habitat fragmentation affect the projected future distribution of European beech. *Global Change Biology*, **21**, 897–910.

Savolainen, O., Pyhäjärvi, T. & Knürr, T. (2007) Gene Flow and Local Adaptation in Trees. *Annual Review of Ecology, Evolution, and Systematics*, **38**, 595–619.

Scheepens, J.F., Deng, Y. & Bossdorf, O. (2018) Phenotypic plasticity in response to temperature fluctuations is genetically variable, and relates to climatic variability of origin, in Arabidopsis thaliana. *AoB PLANTS*, **10**, 1–12.

Stahl, U., Reu, B. & Wirth, C. (2014) Predicting species' range limits from functional traits for the tree flora of North America. *Proceedings of the National Academy of Sciences*, **111**, 13739–13744.

Stojnic, S., Suchocka, M., Benito-Garzon, M., Torres-Ruiz, J., Cochard, H., Bolte, A., Cocozza, C., Cvjetkovic, B., de Luis, M., Martinez-Vilalta, J., Raebild, A., Tognetti, R. & Delzon, S. (2018) Variation in xylem vulnerability to embolism in European beech from geographically marginal populations Variation in xylem vulnerability to embolism in European beech from geographically marginal populations. *Tree Physiology*, **38**, 173–185.

Svenning, J.C. & Skov, F. (2005) The relative roles of environment and history as controls of tree species composition and richness in Europe. *Journal of Biogeography*, **32**, 1019–1033.

Trumbore, S., Brando, P. & Hartmann, H. (2015) Forest health and global change. *Science*, **349**, 814–818.

Urban, M.C., Bocedi, G., Hendry, A.P., Mihoub, J.B., Pe'er, G., Singer, A., Bridle, J.R., Crozier, L.G., De Meester, L., Godsoe, W., Gonzalez, A., Hellmann, J.J., Holt, R.D., Huth, A., Johst, K., Krug, C.B., Leadley, P.W., Palmer, S.C.F., Pantel, J.H., Schmitz, A., Zollner, P.A. & Travis, J.M.J. (2016) Improving the forecast for biodiversity under climate change. *Science*, **353**.

Valladares, F., Matesanz, S., Guilhaumon, F., Araújo, M.B., Balaguer, L., Benito-Garzón, M., Cornwell, W., Gianoli, E., van Kleunen, M., Naya, D.E., Nicotra, A.B., Poorter, H. & Zavala, M.A. (2014) The effects of phenotypic plasticity and local adaptation on forecasts of species range shifts under climate change. *Ecology Letters*, **17**, 1351–1364.

Vautard, R., Gobiet, A., Sobolowski, S., Kjellström, E., Stegehuis, A., Watkiss, P., Mendlik, T., Landgren, O., Nikulin, G., Teichmann, C. & Jacob, D. (2014) The European climate under a 2 ◦ C global warming. *Environmental Research Letters*, **9**, 1–11.

Vitasse, Y., Lenz, A., Hoch, G. & Korner, C. (2014) Earlier leaf-out rather than difference in freezing resistance puts juvenile trees at greater risk of damage than adult trees. *Journal of Ecology*, **102**, 981–988.

Volaire, F. (2018) A unified framework of plant adaptive strategies to drought: crossing scales and disciplines. *Global Change Biology (in press)*.

Way, D.A. & Montgomery, R.A. (2015) Photoperiod constraints on tree phenology, performance and migration in a warming world. *Plant, Cell & Environment*, **38**, 1725–1736.

Younginger, B.S., Sirová, D., Cruzan, M.B. & Ballhorn, D.J. (2017) Is Biomass a Reliable Estimate of Plant Fitness? *Applications in Plant Sciences*, **5**, 1600094.

DATA ACCESSIBILITY

All phenotypic data used in this study are available at https://zenodo.org/record/1240931#.XBuSa81CeUk (Robson *et al.*, 2018). All the maps generated in this study are available from the authors.

Tables & Figures

Figure 1. Map: Distribution range of *Fagus sylvatica* L. (shaded in beige) and location of the provenances and trials by trait. Circles indicate the location of the provenances and triangles that of the trials. Different colors have been employed to indicate the different traits (VG: vertical growth; RG: radial growth; YTS: young tree survival; LF: leaf flushing). Table: The extent of data from the BeechCOSTe52 database (Robson et al. 2018) used for modelling. Measurements: total number of measurements; Trees: total number of individual trees; Trials: total number of trials; Provenances: total number of provenances, Age: the age at which the trees were measured. Columns indicate sample sizes for the traits used in the one-trait models and in the two-trait models.

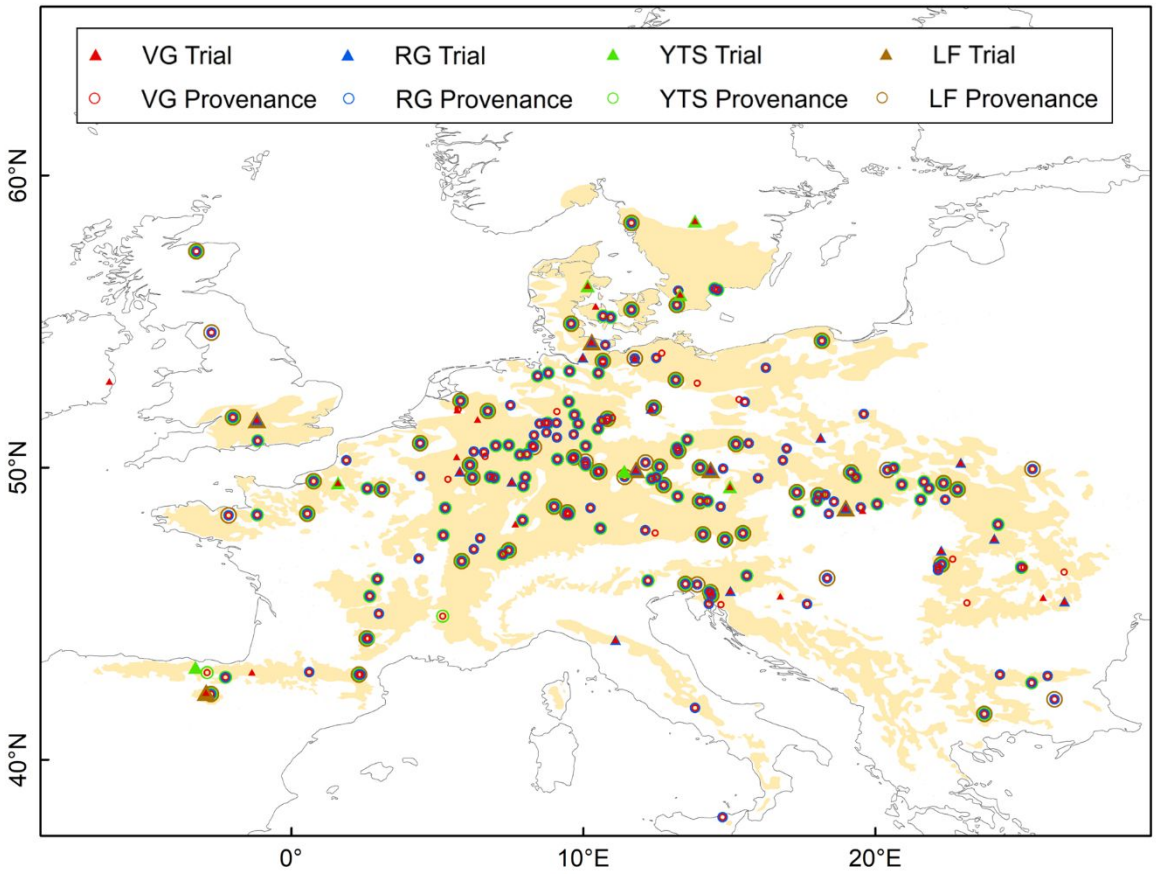

	VG	RG	YTS	LF	H-RG	H-LF
Measurements	203 105	34 237	41 309	7 863	34 237	12 087
Trees	108 415	31 339	37 433	7 863	31 339	10 634
Trials	36	19	7	7	19	6
Provenances	205	186	114	62	186	150
Age	2 to 15	8 to 15	2 to 6	12	8 to 15	6, 9, 11, 12, 15

Table 1. Summary of the variables included in the final best-supported models (one- and two-trait) for each trait analyzed. Environmental variables selected for the provenances and the trials for the one-trait models of height, DBH, young tree survival and flushing, and for the two-trait models of height-DBH and height-leaf flushing. H: height; DBH: diameter at breast height; Lf: leaf flushing; PET Max: maximal monthly potential evapotranspiration; BIO12: annual precipitation; BIO13: precipitation of wettest month; BIO14: precipitation of driest month; MTdjf: mean temperature of December, January and February; Co-variate: trait covariate.

		one-trait models				two-trait models	
		Height	**DBH**	**Young tree survival**	**Leaf flushing**	**H-DBH**	**H-Lf**
Variables	**Environment of the provenance**	PET Max	PET Max	PET Max	MTdjf Latitude	PET Max	PET Max
	Environment of the trial	BIO13	BIO12	BIO14	MTdjf Latitude Longitude	BIO13	BIO13
	Co-variate					DBH	Lf

Table 2. Summary statistics for a generalized linear model (binomial family) of beech occurrence (presence/absence) as a function of trait spatial predictions and their interactions. Estimate: coefficient of the regression shown on a logarithmic scale; SE: standard error of fixed variables; *t*: Wald statistical test that measures the point estimate divided by the estimate of its standard error, assuming a Gaussian distribution of observations; *p*: p-value; DE: deviance explained; VG: vertical growth; RG: radial growth; YTS: young tree survival; LF: leaf flushing.

	Estimate	**SE**	***t***	***p***	**DE**
(Intercept)	-5.84	1.15e-02	-509.03	2.00E-16	
VG	5.45	1.64e-02	332.93	2.00E-16	0.37
RG	0.51	7.93e-03	64.67	2.00E-16	0.33
YTS	2.11	3.75e-03	562.83	2.00E-16	0.19
LG	3.12	1.48e-02	210.94	2.00E-16	0.01
VG x YTS	0.10	4.30e-03	21.08	2.00E-16	0.03
RG x YTS	-0.60	2.04e-03	-295.94	2.00E-16	0.01
YTS x LF	-1.40	4.02e-03	-348.1	2.00E-16	0.01
VG x RG	-1.11	4.62e-03	-240.58	2.00E-16	0.01
VG x LF	-7.81	2.15e-02	-363.18	2.00E-16	0.01
RG x LF	3.43	1.09e-02	313.89	2.00E-16	0.02
Model total deviance					**0.31**

Figure 2. Spatial projections for (a) vertical growth (cm), (b) radial growth (mm), (c) young tree survival (probability) and (d) leaf flushing (Julian days) generated using one-trait models (maps on the left), and corresponding graphs of interactions between the best environmental predictor variable across the trials divided according to environment at the provenance for each of the four traits (graphs on the right). Interactions represent the differences in trait values that can be attributed to the provenance (interpretable as local adaptation driven by PET max in (a), (b), and (c) and driven by the latitude in (d)). Interactions also represent the differences in trait values that can be attributed to the environmental conditions of trial (interpretable as phenotypic plasticity driven by the environmental variables shown in the x-axis). Black, dark grey, and light grey lines represent high, medium and low values of the climatic variable of the provenances (as opposed to those of the trial, indicated on the x-axis). The vertical lines represent the confidence intervals. The maps display the trait projection for contemporary climate (inferred from 2000-2014 meteorological data) across the current species range. The color gradient depicts the clinal variation from low (red) to high (blue) values of each trait. The values of the different traits are represented in the following way: vertical growth (cm), radial growth (mm), probability of young tree survival (0 =dead, 1=alive) and leaf flushing (Julian days). PET max prov: maximal monthly potential evapotranspiration at the provenance; Latitude prov: latitude of the provenance.

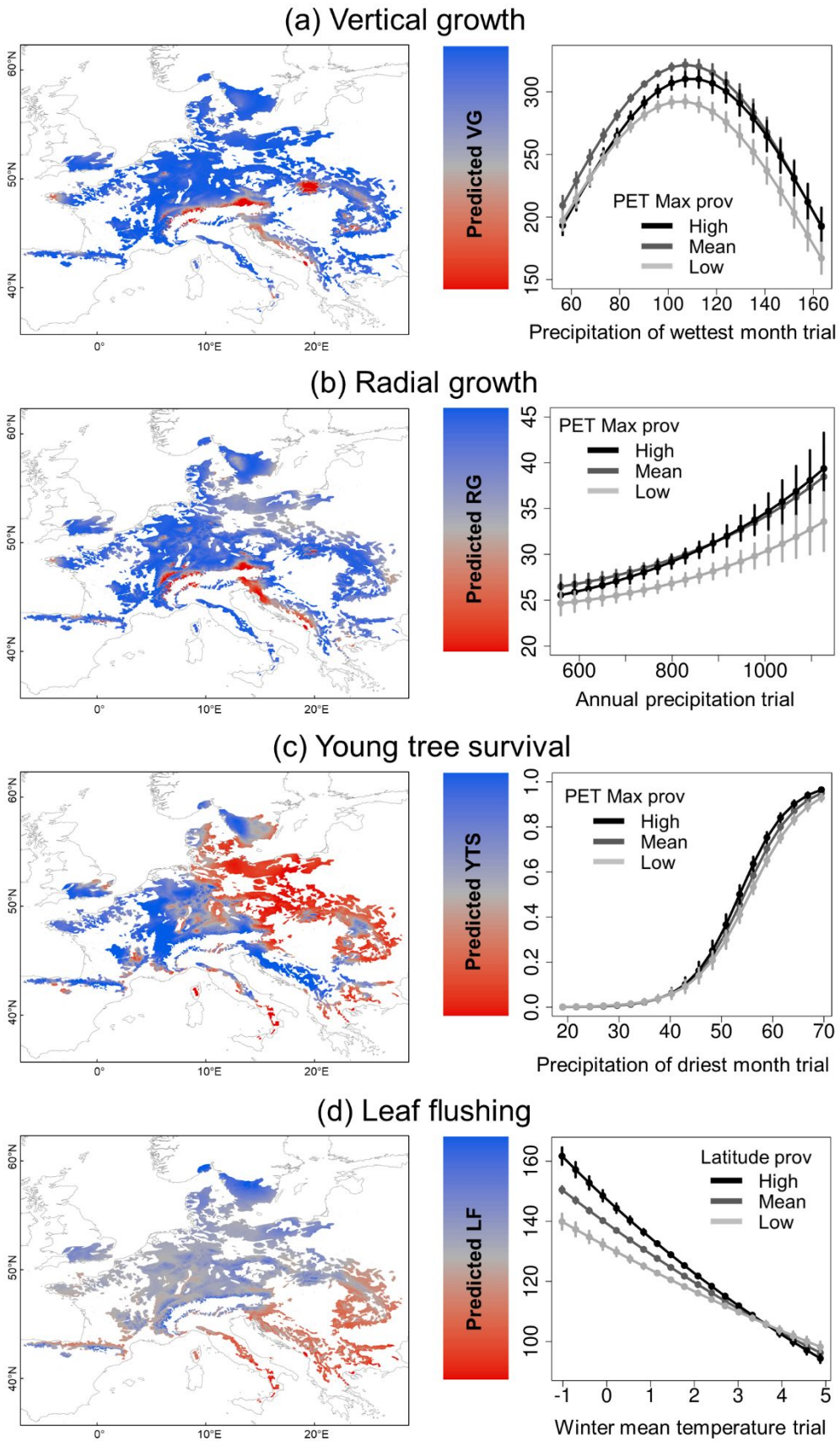
(a) Vertical growth
Predicted VG
PET Max prov
High
Mean
Low
Precipitation of wettest month trial
(b) Radial growth
Predicted RG
PET Max prov
High
Mean
Low
Annual precipitation trial
(c) Young tree survival
Predicted YTS
PET Max prov
High
Mean
Low
Precipitation of driest month trial
(d) Leaf flushing
Predicted LF
Latitude prov
High
Mean
Low
Winter mean temperature trial
60°N
50°N
40°N
0°
10°E
20°E

801

Figure 3. Spatial projections of vertical growth (cm) for (a) Vertical-radial growth model and (b) vertical growth-leaf flushing models (maps on the left), and the corresponding graphs of co-variation between vertical growth and the covariate: (a) DBH (mm) and (b) leaf flushing (Julian days). Black, dark grey, and light grey lines represent high, medium and low values of the precipitation of the wettest month of the trial (BIO13). The vertical lines represent the confidence intervals. The maps display the trait projection for contemporary climate (inferred from 2000-2014 meteorological data) across the current species range. The color gradient depicts the clinal variation in vertical growth from 200 cm (gray) to 600 cm (blue).

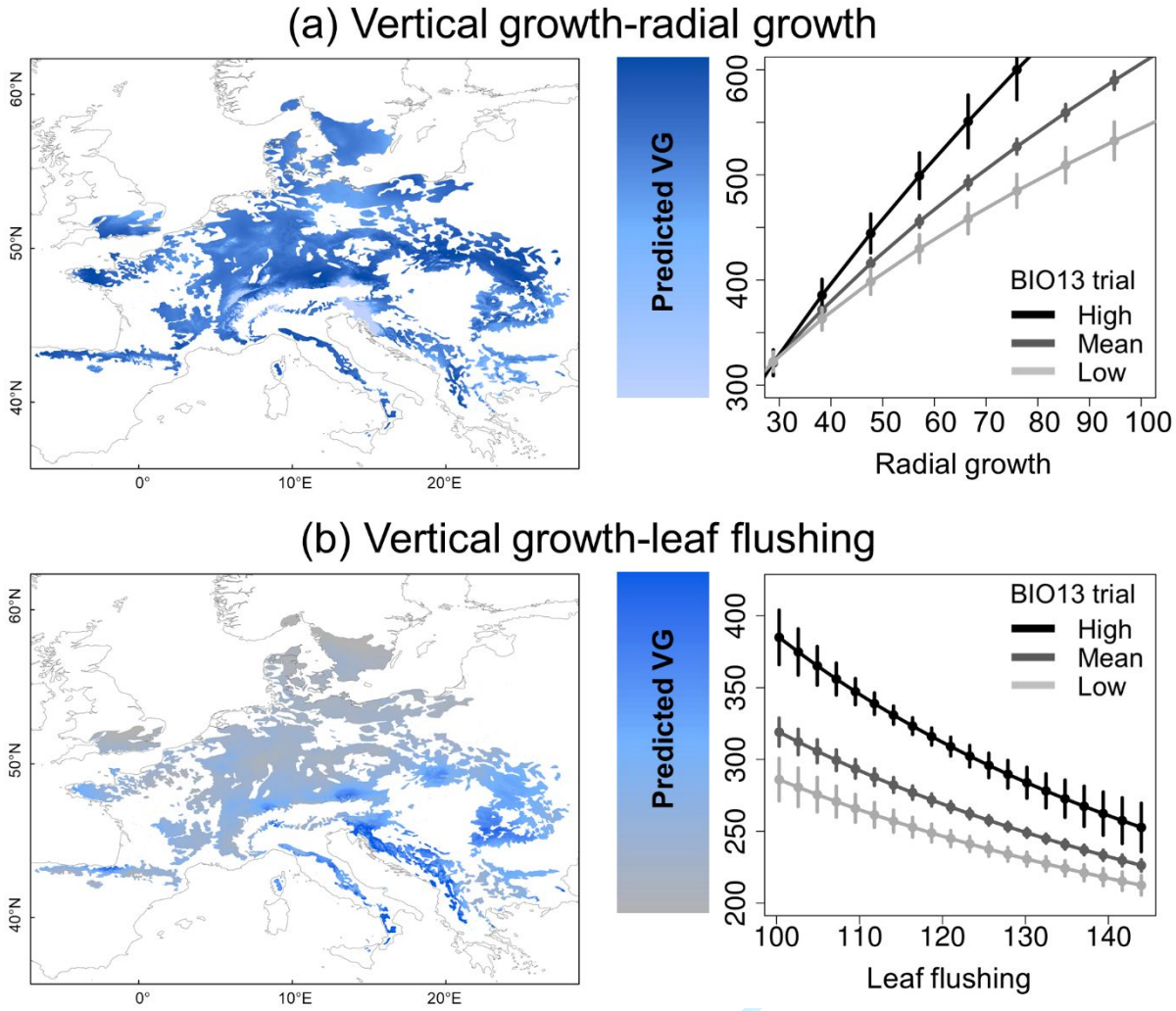

Figure 4. Spatial predictions for 2070 (RCP 8.5) across the species range for one-trait models: (a) vertical growth (cm); (b) radial growth (mm); (c) probability of young tree survival (0=dead; 1=alive); (d) leaf flushing (Julian days); and for two-trait models: (e) vertical growth (cm; co-variate radial growth) and (f) vertical growth (cm; co-variate leaf flushing). The color gradients depict the clinal variation from low (red) to high (blue) values.

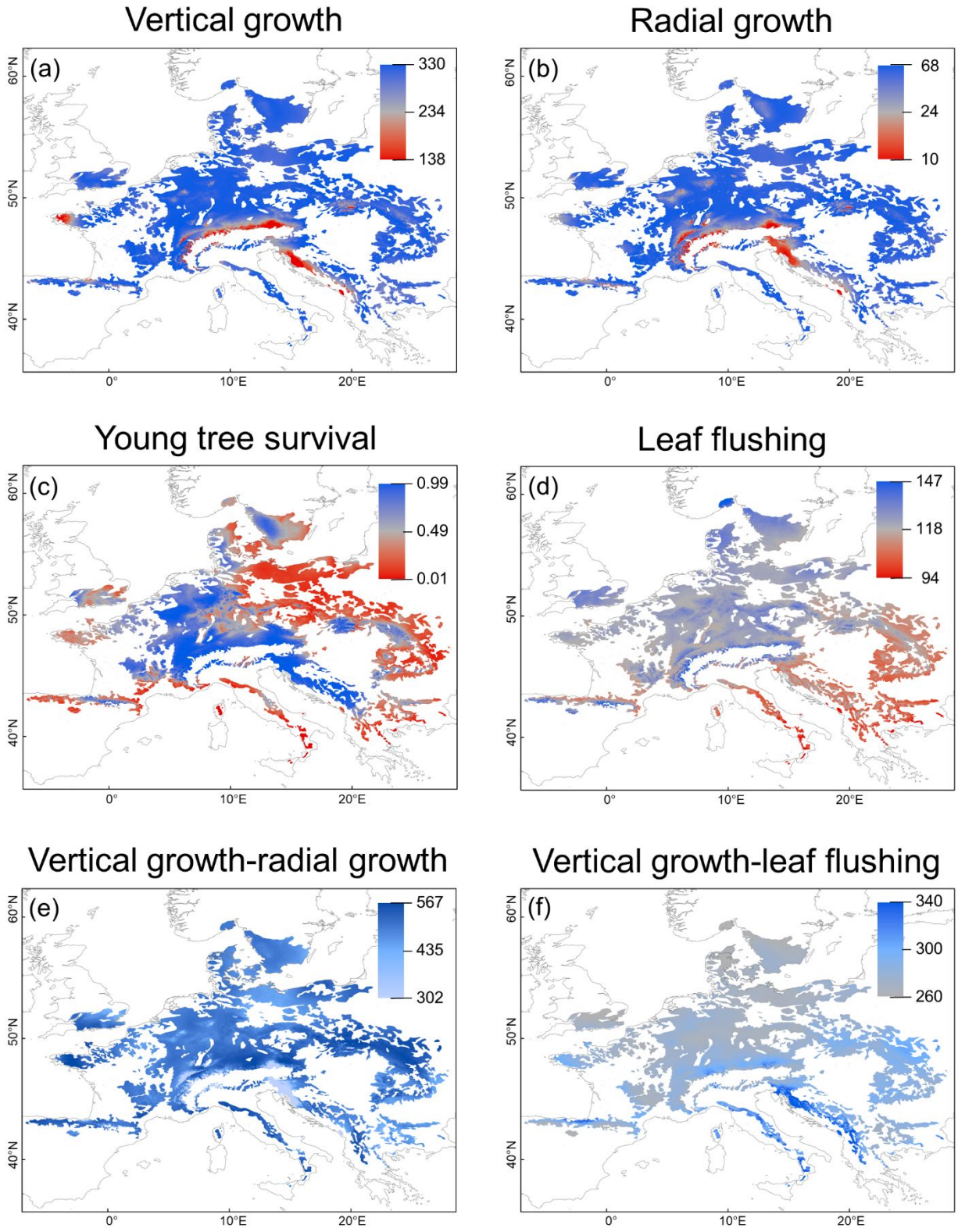
Vertical growth
(a)
330
234
138
Radial growth
(b)
68
24
10
Young tree survival
(c)
0.99
0.49
0.01
Leaf flushing
(d)
147
118
94
Vertical growth-radial growth
(e)
567
435
302
Vertical growth-leaf flushing
(f)
340
300
260
60°N
50°N
40°N
0°
10°E
20°E

820

APPENDIX S1: Supporting information

1. Moran's I correlation coefficient

Supporting Information Table S1.1. Statistics of the spatial autocorrelation of vertical growth (VG), radial growth (RG), young tree survival (YTS) and leaf flushing (LF). Ob: observed computed Moran's I; Ex: expected value of I under the null hypothesis; Sd: standard deviation of I under the null hypothesis; p-value: p-value of the test of the null hypothesis against the alternative hypothesis; Null hypothesis: the data does not have spatial correlation.

	VG	RG	YTS	LF
Ob	-0.04	-0.09	-0.17	-0.10
Ex	-0.03	-0.05	-0.13	-0.08
Sd	0.06	0.06	0.17	0.08
p-value	0.81	0.47	0.78	0.74

2. Moran's I correlograms

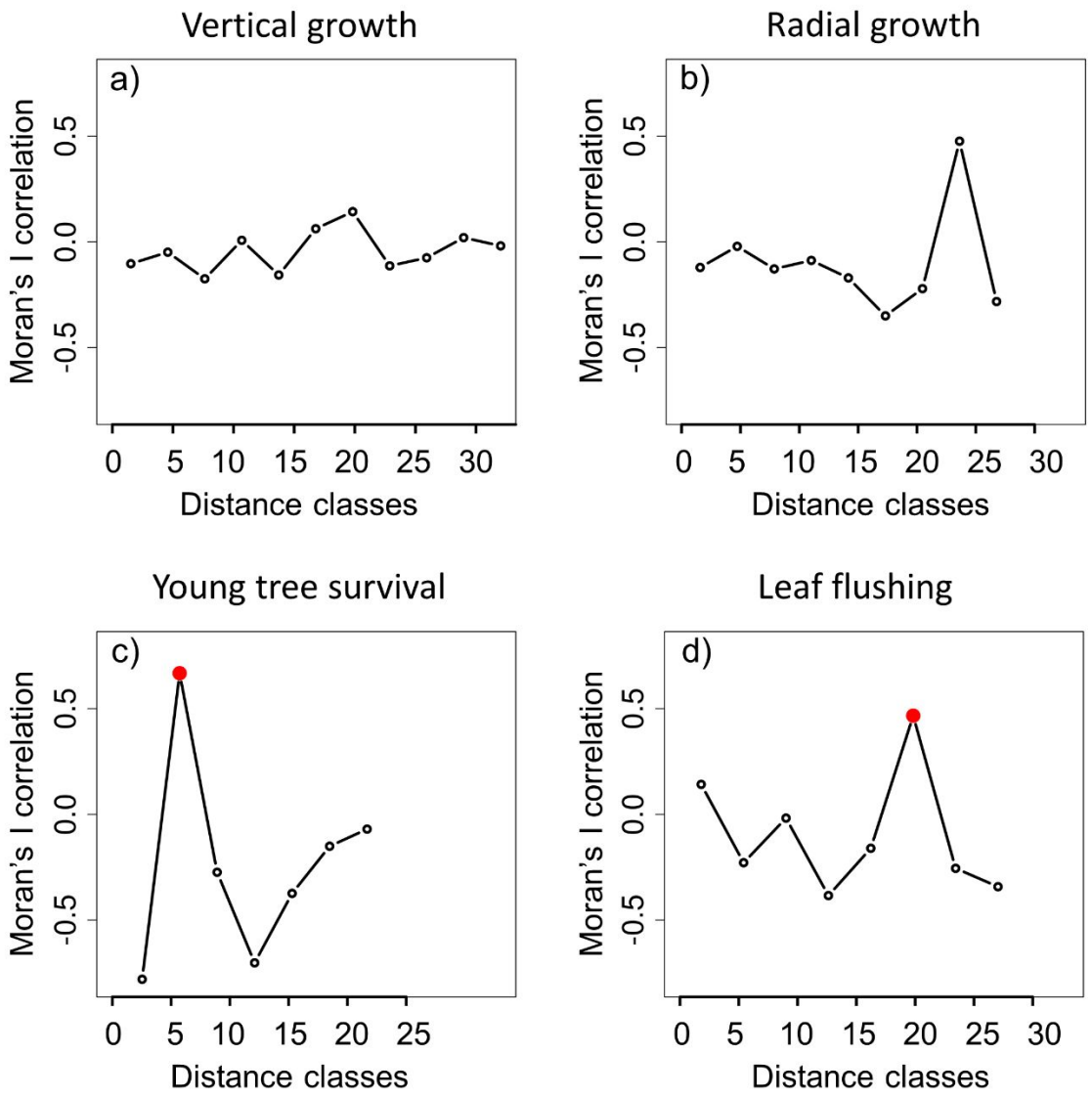

Supporting Information Figure S1.1. Correlograms of Moran's I correlation coefficient (y-axis) and the distance classes (x-axis) for vertical (a) and radial (b) growth, young tree survival (c), and leaf flushing (d). Moran's correlation coefficient ranges between 1 and -1. Distance classes are Euclidian and in degrees. Distances of significant spatial dependence are shown in red (significant values $p < 0.05$).

3. Climatic variables

Supporting Information Table S1.2. List of yearly climatic variables provided by EuMedClim. °C: Celsius degree; mm: millimeters; water balance: precipitation minus potential evapotranspiration.

Climatic variables	Definition	Unit
BIO1	Annual mean temperature	°C
BIO2	Mean diurnal temperature range	°C
BIO5	Maximal temperature of the warmest month	°C
BIO6	Minimal temperature of the coldest month	°C
BIO12	Annual precipitation	mm
BIO13	Precipitation of the wettest month	mm
BIO14	Precipitation of the driest month	mm
MTdjf	Mean temperature of December, January and February	°C
MTmam	Mean temperature of March, April and May	°C
MTjaj	Mean temperature of June, July and August	°C
MTson	Mean temperature of September, October and November	°C
Pdjf	Precipitation of December, January and February	mm
Pmam	Precipitation of March, April and May	mm
Pjaj	Precipitation of June, July and August	mm
Pson	Precipitation of September, October and November	mm
PET Mean	Annual potential evapotranspiration	mm
PET Max	Maximal monthly potential evapotranspiration	mm
PET Min	Minimal monthly potential evapotranspiration	mm
PPET Mean	Annual water balance	mm
PPET Max	Maximal monthly water balance	mm
PPET Min	Minimal monthly water balance	mm

4. Principal Components Analysis (PCA) of the climate variables

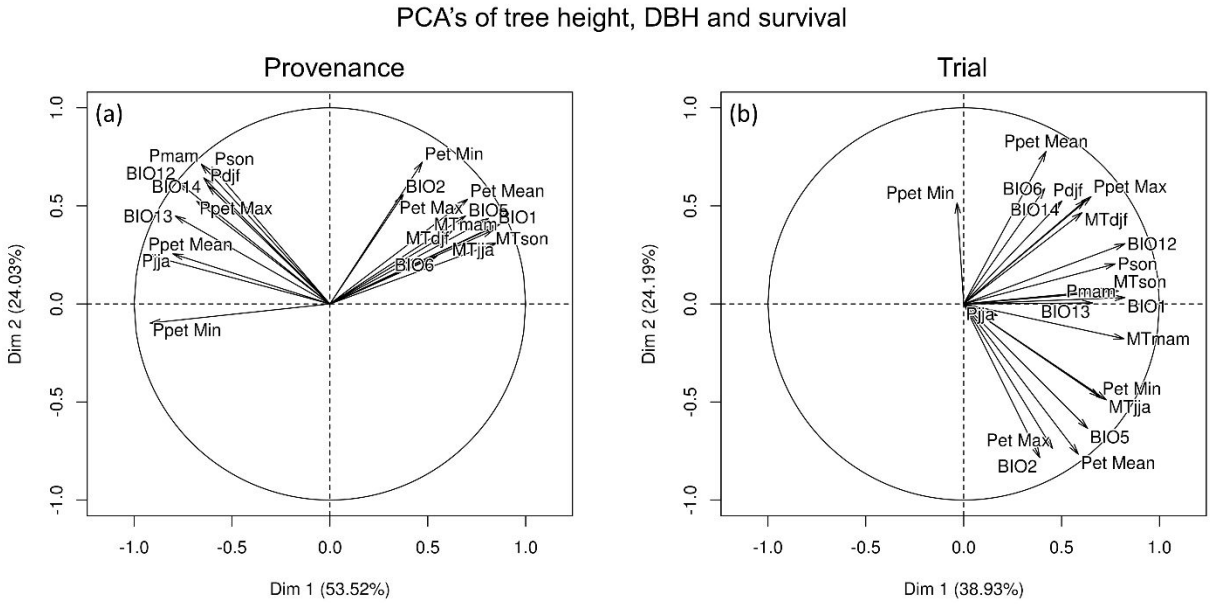

Supporting Information Figure S1.2. Results of PCA for checking for co-linearity and reducing the climatic space to select the final climate variables for the stepwise procedure used in the models on traits vertical and radial growth, and young tree survival, conducted by provenance (a) and by trial (b). When two variables are strongly correlated, only one of them was used in models. The variance explained by the first two axes is indicated in the figures.

5. AIC analysis

We performed a total of 64 one-trait models and selected the best model based on AIC.

Supporting Information Table S1.3. AIC values obtained for vertical growth, radial growth, young tree survival and leaf flushing one-trait models. AIC: Akaike information criterion; CP: climate of the provenance; CT: climate of the trial; BIO1: annual mean temperature; BIO5: max temperature of warmest month; BIO6: min temperature of coldest month; BIO12: annual precipitation; BIO13: precipitation of wettest month; BIO14: precipitation of driest month; PET Max: maximal monthly potential evapotranspiration; PET Mean: annual potential evapotranspiration; MTdjf: mean temperature of December, January and February; MTmam: mean temperature of March, April and May; MTjja: mean temperature of June, July and August; MTson: mean temperature of September, October and November; MTdjfmam: mean temperature of December, January, February March, April and May.

Vertical growth			Radial growth			Young tree survival			Leaf flushing		
CP	CT	AIC	CP	CT	AIC	CP	CT	AIC	CP	CT	AIC
PET Max	BIO13	102495.10	PET Max	BIO12	23099.69	PET Max	BIO14	39299.61	MTdjf	MTdjf	-32835.88
BIO13	BIO13	102498.40	BIO12	BIO12	23099.77	BIO5	PET Max	39299.75	MTdjfmam	BIO5	-32835.2
BIO1	BIO13	102509.20	PET Mean	BIO12	23100.00	BIO5	BIO13	39300.20	MTdjfmam	MTdjf	-32835.01
BIO5	BIO13	102509.70	BIO5	BIO12	23100.17	BIO14	BIO14	39300.57	MTdjf	BIO5	-32834.71
PET Mean	BIO13	102515.30	BIO13	BIO12	23105.95	PET Mean	PET Max	39301.21	BIO1	MTdjf	-32833.53
BIO12	BIO13	102538.90	BIO14	BIO12	23107.76	PET Mean	BIO14	39303.74	MTson	MTdjf	-32833.2
BIO6	BIO13	102647.10	BIO1	BIO12	23109.40	PET Max	PET Max	39307.04	BIO1	BIO5	-32832.97
BIO14	BIO13	102694.40	BIO14	PET Max	23112.39	BIO12	BIO14	39307.83	MTdjfmam	MTjja	-32832.95
BIO5	BIO12	102827.20	BIO6	BIO12	23113.15	BIO5	BIO12	39308.26	BIO6	MTdjf	-32832.8
BIO1	BIO12	102836.50	PET Max	PET Max	23119.66	BIO13	BIO13	39308.30	MTdjf	MTjja	-32832.59
PET Max	BIO12	102849.60	BIO12	PET Max	23119.73	PET Mean	BIO1	39308.32	MTson	BIO5	-32832.53
PET Mean	BIO12	102849.80	PET Mean	PET Max	23123.73	BIO5	BIO14	39308.80	BIO6	BIO5	-32831.78
BIO13	BIO12	102856.00	BIO13	PET Max	23124.58	PET Mean	PET Mean	39308.84	BIO1	MTjja	-32830.75
BIO12	BIO12	102924.80	BIO5	PET Max	23127.81	BIO5	BIO1	39308.93	MTson	MTjja	-32830.39
BIO6	BIO12	103000.30	BIO6	PET Max	23129.06	BIO5	PET Mean	39309.13	MTmam	MTdjf	-32829.82
BIO14	BIO12	103035.00	BIO1	PET Max	23131.01	BIO13	PET Max	39310.60	MTmam	BIO5	-32829.69
BIO13	BIO14	104366.60	PET Mean	BIO13	23155.46	PET Mean	BIO5	39310.84	BIO6	MTjja	-32829.67

BIO12	BIO14	104433.70	BIO1	BIO13	23158.17	BIO13	BIO14	39311.05	MTdjfmam	MTson	-32828.93
BIO5	BIO5	104479.60	BIO5	BIO13	23158.45	PET Mean	BIO13	39311.74	MTdjf	MTson	-32828.49
BIO1	BIO5	104486.20	PET Max	BIO13	23160.20	PET Max	BIO13	39312.16	MTmam	MTjja	-32827.31
BIO13	BIO5	104486.40	BIO6	BIO13	23161.55	BIO13	BIO12	39312.17	BIO1	MTson	-32826.31
PET Max	BIO5	104498.00	BIO12	BIO13	23170.84	BIO6	BIO13	39312.88	BIO5	BIO5	-32826.25
PET Mean	BIO5	104502.00	BIO14	BIO13	23170.94	PET Max	BIO1	39313.22	MTson	MTson	-32825.79
BIO12	BIO5	104531.00	BIO13	BIO13	23172.87	BIO14	BIO13	39313.52	BIO6	MTson	-32825.65
BIO1	BIO14	104548.20	BIO12	BIO14	23213.00	BIO5	BIO6	39313.96	BIO5	MTdjf	-32825.32
BIO6	BIO5	104551.90	BIO13	BIO14	23214.59	BIO12	PET Max	39314.37	BIO5	MTjja	-32824.01
PET Max	BIO14	104554.10	BIO14	BIO14	23221.30	BIO12	BIO13	39314.57	MTmam	MTson	-32823.39
PET Mean	BIO14	104561.80	PET Max	BIO14	23228.03	BIO13	BIO1	39314.63	MTdjfmam	BIO1	-32821.39
BIO5	BIO14	104568.60	BIO12	BIO6	23228.43	BIO5	BIO5	39315.15	MTdjf	BIO1	-32821.3
BIO14	BIO5	104595.80	PET Mean	BIO14	23229.18	PET Max	PET Mean	39315.57	BIO5	MTson	-32819.16
BIO14	BIO14	104632.90	BIO13	BIO6	23230.85	BIO1	BIO13	39315.98	BIO1	BIO1	-32818.88
BIO6	BIO14	104662.10	BIO5	BIO14	23231.28	BIO1	BIO14	39316.04	MTson	BIO1	-32818.63
BIO5	BIO1	104948.50	BIO6	BIO14	23231.86	BIO6	BIO14	39316.50	MTjja	BIO5	-32818.54
PET Max	BIO1	104951.50	BIO1	BIO14	23235.69	BIO12	BIO1	39316.56	BIO6	BIO1	-32818.38
PET Mean	BIO1	104953.40	BIO14	BIO6	23236.45	PET Mean	BIO12	39316.71	MTjja	MTdjf	-32817.94
BIO13	BIO1	104958.20	BIO6	BIO6	23240.51	BIO6	BIO12	39316.72	MTjja	MTjja	-32816.41
BIO1	BIO1	104990.00	PET Max	BIO6	23247.34	BIO6	PET Max	39316.79	MTmam	BIO1	-32815.09
BIO12	BIO1	105034.80	PET Mean	BIO6	23248.79	PET Max	BIO12	39316.82	MTdjfmam	BIO6	-32813.73
BIO6	BIO1	105103.40	BIO5	BIO6	23251.22	BIO13	PET Mean	39317.10	MTdjf	BIO6	-32813.64
BIO14	BIO1	105134.00	BIO1	BIO6	23251.39	PET Max	BIO6	39317.35	MTson	BIO6	-32811.78
BIO13	PET Mean	105607.20	PET Max	BIO5	23326.60	BIO1	PET Max	39317.45	BIO1	BIO6	-32811.7
BIO13	BIO6	105655.60	PET Mean	BIO5	23330.74	PET Max	BIO5	39317.56	MTjja	MTson	-32811.33
BIO12	PET Mean	105700.20	BIO5	BIO5	23333.80	BIO13	BIO6	39317.60	BIO6	BIO6	-32810.51
BIO12	BIO6	105740.90	BIO14	BIO5	23336.46	PET Mean	BIO6	39317.70	BIO5	BIO1	-32810.39
BIO5	PET Mean	105752.70	BIO12	BIO5	23337.86	BIO1	BIO1	39317.71	MTmam	BIO6	-32807.09
BIO1	PET Mean	105753.10	BIO13	BIO5	23342.73	BIO14	PET Max	39317.82	MTjja	BIO1	-32803.17
PET Max	PET Mean	105762.50	BIO1	BIO5	23343.08	BIO14	BIO1	39317.95	BIO5	BIO6	-32803.03
PET Mean	PET Mean	105769.40	BIO12	BIO1	23344.66	BIO14	BIO12	39318.04	MTdjfmam	MTdjfmam	-32798.69
PET Max	BIO6	105777.20	PET Max	BIO1	23345.37	BIO12	BIO12	39318.24	MTdjf	MTdjfmam	-32798.47
PET Mean	BIO6	105777.90	BIO6	BIO5	23345.84	BIO6	BIO1	39318.36	MTson	MTdjfmam	-32796.38
BIO5	BIO6	105782.20	BIO5	BIO1	23349.97	BIO13	BIO5	39318.74	BIO1	MTdjfmam	-32796.37
BIO1	BIO6	105790.00	PET Mean	BIO1	23350.61	BIO12	BIO6	39320.02	MTjja	BIO6	-32795.95
BIO6	PET Mean	105851.70	BIO14	BIO1	23353.91	BIO12	PET Mean	39320.05	BIO6	MTdjfmam	-32795.67
BIO14	PET Mean	105867.10	BIO13	BIO1	23354.27	BIO14	BIO6	39320.34	MTmam	MTdjfmam	-32792.13
BIO6	BIO6	105898.10	BIO6	BIO1	23363.77	BIO6	BIO6	39320.41	BIO5	MTdjfmam	-32787
BIO14	BIO6	105901.40	BIO1	BIO1	23367.18	BIO12	BIO5	39320.73	MTdjfmam	MTmam	-32786.71
BIO13	PET Max	106062.80	BIO14	PET mean	23417.15	BIO1	BIO6	39321.01	MTdjf	MTmam	-32785.98
BIO12	PET Max	106132.40	PET Max	PET mean	23420.69	BIO1	BIO12	39321.06	BIO1	MTmam	-32784.65
BIO1	PET Max	106176.20	BIO12	PET mean	23423.00	BIO1	PET Mean	39321.28	MTson	MTmam	-32784.57
BIO5	PET Max	106179.00	PET Mean	PET mean	23423.23	BIO6	PET Mean	39321.81	BIO6	MTmam	-32783.62
PET Max	PET Max	106187.20	BIO5	PET mean	23426.95	BIO14	PET Mean	39321.88	MTmam	MTmam	-32780.58
PET Mean	PET Max	106194.00	BIO13	PET mean	23427.90	BIO14	BIO5	39322.35	MTjja	MTdjfmam	-32780.05
BIO14	PET Max	106256.90	BIO6	PET mean	23431.24	BIO1	BIO5	39323.48	BIO5	MTmam	-32775.52
BIO6	PET Max	106268.70	BIO1	PET mean	23432.28	BIO6	BIO5	39323.84	MTjja	MTmam	-32768.2

6. Summary statistics of one-trait models

Supporting Information Table S1.4. Statistics of random and fixed effects from generalized linear mixed-effect models of vertical growth, radial growth, young tree survival and leaf flushing. Obs: number of trait measurements; Variance: variance explained by the random effects; SD: standard deviation of each level of random effects; Estimate: coefficient of the regression, shown on a logarithmic scale for vertical growth, radial growth and leaf flushing; SE: standard error of each fixed variable; *t*: Wald statistical test that measures the point estimate divided by the estimate of its SE, assuming a Gaussian distribution of observations conditional on fixed and random effects; *z*: Wald statistical test that measures the point estimate divided by the estimate of its SE, assuming a binomial distribution of observations conditional on fixed and random effects. Fixed effects: Coefficients of the fixed effects of the model; CP: climate of the provenance origin; CT: climate of the trial; LatP: latitude of the provenance origin; LatT: latitude of the trial; LongT: longitude of the trial; CP^2: quadratic effect of the climate of the provenance; CT^2: quadratic effect of the climate of the trial. Coefficients of the interactions: Age x CP, Age x CT, CP x CT, LatP x CT, LatP x LatT, LatP x LongT, CP x LongT. R^2M: percentage of the variance explained by the fixed effects (Marginal variance); R^2C: percentage of the variance explained by the random and fixed effects (Conditional variance); r: Pearson correlation. The climate variable of the provenance (CP) for vertical growth, radial growth and young tree survival is maximal potential evapotranspiration; CP for leaf flushing is mean temperature of December, January and February. The climate variable of the trial (CT) for vertical growth is precipitation of the wettest month, for radial growth is annual precipitation, for young tree survival is precipitation of the driest month and for leaf flushing is mean temperature of December, January and February.

	Vertical growth			**Radial growth**			**Young tree survival**			**Leaf flushing**		
Model	Linear Mixed Effect			Linear Mixed Effect			Generalized Linear Mixed Effect (Family: binomial)			Linear Mixed Effect		
	Random Effects			Random Effects			Random Effects			Random Effects		
	Obs	Variance	SD	Obs	Variance	SD	Obs	Variance	SD	Obs	Variance	SD
Provenance	205	1.00e-02	9.00e-02	187	9.31e-03	9.65e-02	114	2.98e-01	5.46e-01	62	4.60e-04	2.20e-02
Trial	36	9.00e-02	3.00e-01	19	3.81e-01	6.17e-01	7	6.31e-01	7.94e-01	7	3.60e-05	6.00e-03
Trial:Block	107	9.00e-02	1.00e-01	56	6.97e-03	8.35e-02	21	1.48e-01	3.84e-01			
Trial:Block:Tree	108415	8.00e-02	2.80e-01	31339	1.10e-01	3.32e-01	37433	1.16e-02	1.08e-01			
Residuals		5.00e-02	2.20e-01		1.66e-02	1.29e-01		1.54e-01	3.92e-01		8.56e-04	2.92e-02
	Fixed Effects			Fixed Effects			Fixed Effects			Fixed Effects		
	Estimate	SE	*t*	Estimate	SE	*t*	Estimate	SE	*z*	Estimate	SE	*t*
Intercept	4.84e+00	5.22e-02	92.7	2.82e+00	1.56e-01	18.1	1.08e+00	3.38e-01	3.2	4.76e+00	5.16e-03	921.9
Age	6.45e-01	1.14e-03	563.6	7.17e-01	8.74e-03	82	-1.72e+00	9.29e-02	-18.5			
CP	2.58e-02	6.93e-03	3.7	2.94e-02	8.81e-03	3.3	2.83e-02	5.30e-02	0.1	1.07e-02	2.63e-03	4.1
CT	9.70e-02	4.63e-03	20.9	2.54e-01	7.02e-02	3.6	1.54e-01	2.78e-01	0.6	-1.28e-01	9.77e-03	-13.1
LatP										5.43e-03	2.63e-03	2.1
LatT										4.38e-02	4.77e-03	9.2
LongT										-1.12e-01	9.87e-03	-11.4
CP^2	-1.27e-02	4.84e-03	-2.6									
CT^2	-1.50e-01	2.45e-03	-61.2	-4.30e-01	5.89e-02	-7.3						
Age x CP	-1.07e-02	7.86e-04	-13.6	-1.09e-02	3.58e-03	3						
Age x CT	-1.92e-02	1.50e-03	-12.8	3.33e-01	1.44e-02	23.1	1.59e+00	1.21e-01	13.1			
CP x CT	9.58e-03	1.29e-03	7.4	7.45e-03	3.01e-03	2.5	8.11e-02	2.52e-02	3.2			
LatP x CT										-1.08e-02	1.74e-03	-6.2
LatP x LatT										4.15e-03	7.95e-04	5.2
LatP x LongT										-1.09e-02	1.61e-03	-5.3
CP x LongT										-2.63e-03	4.98e-04	-6.8
	r	R^2 M	R^2 C	r	R^2 M	R^2 C	r	R^2 M	R^2 C	r	R^2 M	R^2 C
	0.69	0.57	0.91	0.53	0.51	0.98	0.59	0.18	0.40	0.73	0.49	0.68

7. Summary statistics of two-trait models

Supporting Information Table S1.5. Statistics of random and fixed effects from linear mixed-effect models of the vertical growth-radial growth and vertical growth-leaf flushing two-trait models. Obs: number of trait measurements; Variance: variance explained by the random effects; SD: standard deviation of each level of random effects; Estimate: coefficient of the regression shown in logarithmic scale; SE: standard error of each fixed variable; *t*: Wald statistical test that measures the point estimate divided by the estimate of its SE, assuming a Gaussian distribution of observations conditional on fixed and random effects. Coefficients of the fixed effects of the model: Cov: trait covariate; CP: climate of the provenance origin; CT: climate of the trial; CP^2: quadratic effect of the climate of the provenance. Coefficients of the interactions: Age x CP, CP x CT, Cov x Age and Cov x CT. R^2M: percentage of the variance explained by the fixed effects (Marginal variance); R^2C: percentage of the variance explained by the random and fixed effects (Conditional variance); *r*: Pearson correlation. The trait co-variate (Cov) for growth-radial growth is radial growth and for vertical growth-leaf flushing is leaf flushing. The climate variable of the trial (CT) for the two-trait models is precipitation of the wettest month (BIO13). The climate variable of the provenance (CP) for the two-trait model is maximal potential evapotranspiration.

	Vertical growth-Radial growth			**Vertical growth-Leaf flushing**		
Model	Linear Mixed Effect			Linear Mixed Effect		
	Random Effects			Random Effects		
	Obs	Variance	SD	Obs	Variance	SD
Provenance	187	1.70e-03	4.21e-02	150	2.33e-02	1.53e-01
Trial	19	3.26e-02	1.81e-01	6	1.05e-01	3.24e-01
Trial:Block	56	2.20e-03	4.60e-02	17	1.00e-03	3.24e-02
Trial:Block:Tree	31339	9.50e-03	9.70e-02	10634	9.82e-02	3.13e-01
Residuals		1.50e-02	1.23e-01		2.70e-03	5.21e-02
	Fixed Effects			Fixed Effects		
	Estimate	SE	*t*	Estimate	SE	*t*
Intercept	4.38E+00	4.51e-02	97.18	4.94e+00	4.23e-01	11.68
Cov	3.50E-01	5.02e-03	69.72	6.24e-02	8.40e-02	0.74
Age	-1.97E-01	1.26e-02	-15.66	7.40e+00	5.28e-01	14.01
CP	5.04E-03	3.47e-03	1.45	2.59e-02	1.38e-02	1.87
CT	-1.33E-01	3.47e-02	-3.84	1.91e+00	3.89e-01	4.92
CP^2	-5.26E-03	2.43e-03	-2.17			
Age x CP				-1.96e-02	5.33e-03	-3.68
CP x CT	-3.47E-02	9.66e-03	-3.59	1.78e-02	5.72e-03	3.11
Cov x Age	1.05E-01	3.44e-03	30.57	-1.43e+00	1.09e-01	-13.08
Cov x CT	8.02E-02	3.82e-03	21	-3.84e-01	7.84e-02	-4.89
	r	R^2 M	R^2 C	*r*	R^2 M	R^2 C
	0.76	0.62	0.95	0.77	0.47	0.99

8. Differences in spatial predictions between future and current climate for one- and two-trait models

Vertical growth prediction for 12 year-old trees showed small changes in the core of the species range, and moderate decrease in growth in some areas of southern, eastern, western and northern Europe. Increases in vertical growth were mainly expected in the eastern region of the distribution (Supporting Information Figure S1.3a, Appendix S1). Radial growth of 12 year-old trees was predicted to increase in the eastern regions and to decrease across the rest of the range (Supporting Information Figure S1.3b, Appendix S1). Survival of 6 year-old trees was expected to strongly decrease in the western and southern parts of the distribution. Increases in young tree survival were mainly expected in central and some eastern regions of the species range (Supporting Information Figure S1.3c, Appendix S1). The model predicted later leaf flushing in the future than at present for almost all central and western parts of the species distribution. Earlier leaf flushing in the future than today was particularly expected in Sweden (Supporting Information Figure S1.3d, Appendix S1). Differences in vertical growth predictions between future and present climatic conditions for the vertical growth-radial growth model showed an overall increase in vertical growth in some regions of the eastern and southern range; the largest decrease was expected in the southeastern region (Supporting Information Figure S1.3e, Appendix S1). Differences in vertical-growth predictions between the future and present conditions for the vertical growth-leaf flushing model anticipated a decrease in the southeastern and the southern range. A small increase in the northeast was predicted by this model (Supporting Information Figure S1.3f, Appendix S1).

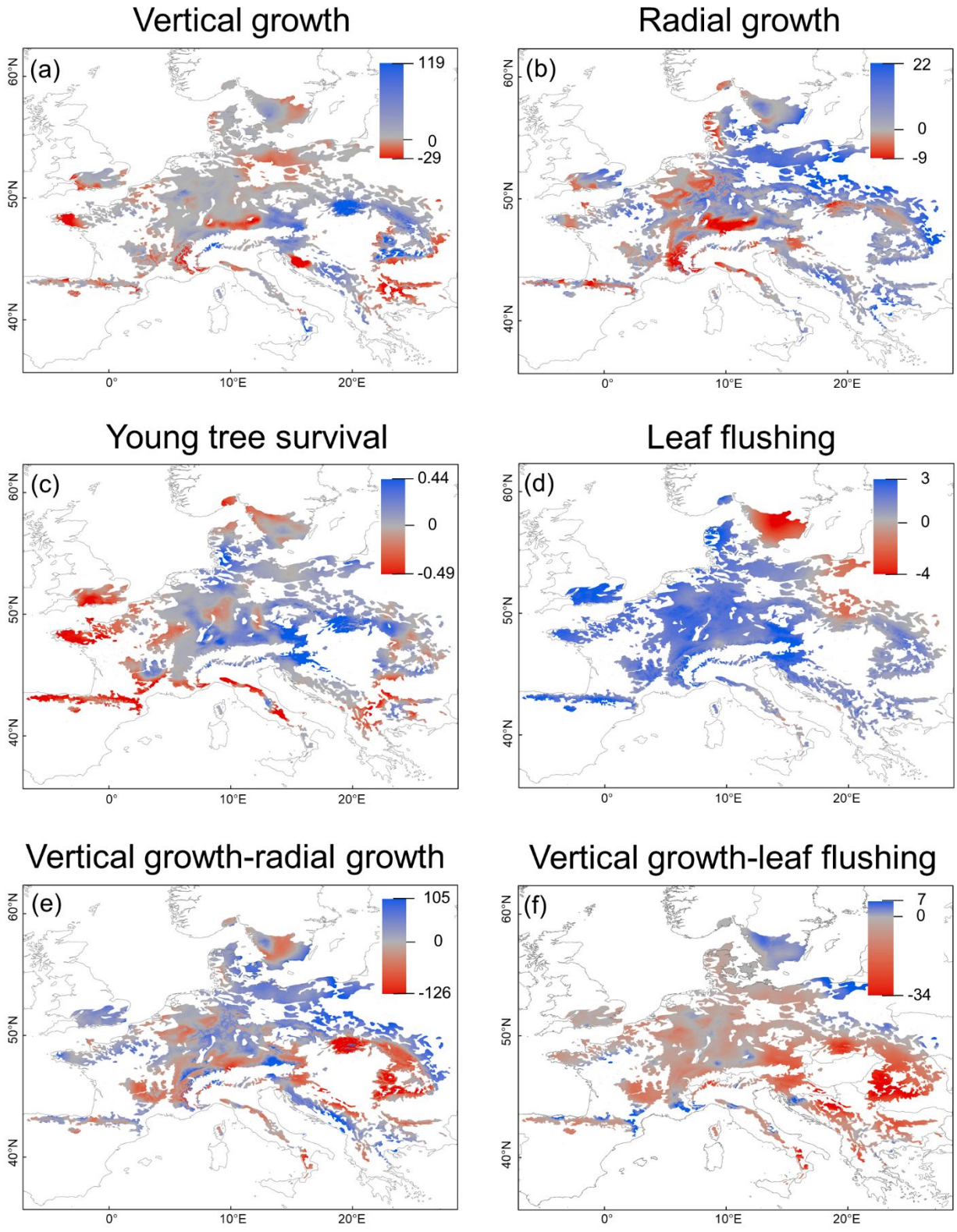
Vertical growth
(a)
119
0
-29
Radial growth
(b)
22
0
-9
Young tree survival
(c)
0.44
0
-0.49
Leaf flushing
(d)
3
0
-4
Vertical growth-radial growth
(e)
105
0
-126
Vertical growth-leaf flushing
(f)
7
0
-34
60°N
50°N
40°N
0°
10°E
20°E

Supporting Information Figure S1.3. Differences in predictions between future (2070) and contemporary (2000-2014) climate for one-trait models in beech range: (a) vertical growth of 12 year-old trees (in cm); (b) radial growth of 12 year-old trees (in mm); (c) probability of young tree survival of 6 year-old trees; (d) leaf flushing of 12 year-old trees (difference in Julian days); and for two-trait models: (e) vertical growth (in cm; co-variate radial growth) and (f) vertical growth (in cm; co-variate leaf flushing). The color gradient depicts the clinal variation from low (red) to high (blue) values.

Dear Editors,

Many thanks again for the review, we addressed all the minor points raised by the editors and one of the reviewers.

Yours sincerely,

Marta Benito Garzón on behalf of the co-authors

EDITOR'S COMMENTS TO AUTHORS
Editor: Blonder, Benjamin
Comments to the Author:
The authors have assessed the substance of all of the reviewers' and my points. The work is likely to be of broad interest to our readership. I think the manuscript is essentially ready to go. There are only a few minor presentation issues remaining that could be trivially addressed by the authors:

R: Many thanks for checking and editing the manuscript, we followed all your advises in our reviewed version of the manuscript.

Abstract: I would rather say that one of the main conclusions is that the drivers of range limits are dependent on trait x environment interactions - not only do multiple traits matter, but each trait matters differently depending on the environmental variable.
R: Thank you, we agree and changed the sentence accordingly.

103: broadleaf, not broadleaved
R: Changed
221: delta term is not clear, suggest replacing with ΔAIC
R: Changed
488: based on, not based in
R: Changed
506: this is a run-on sentence - please fix.
R: We split this sentence in two.
510: could, not can

Changed

Figure 1: can you make symbols in the inset legend larger? They are hard to see.

We made larger the symbols of the inset, thank you.

Figure 2/4: please consider replacing color scales with more colorblind-friendly version, e.g. just a simple red-gray-blue gradient (no yellow or green)

R: Thank you, we changed them to a red-gray-blue scale.

Referee: 2

I am happy that my comments were useful for this manuscript. Just a note, in this sentence: "[...in certain parts of the southern and eastern range of beech, reflecting the climatic marginality due to continentality of the species in these areas...]", you perhaps refer to continentality of the climate, and not of the species.

R: Thank you, we fixed it.

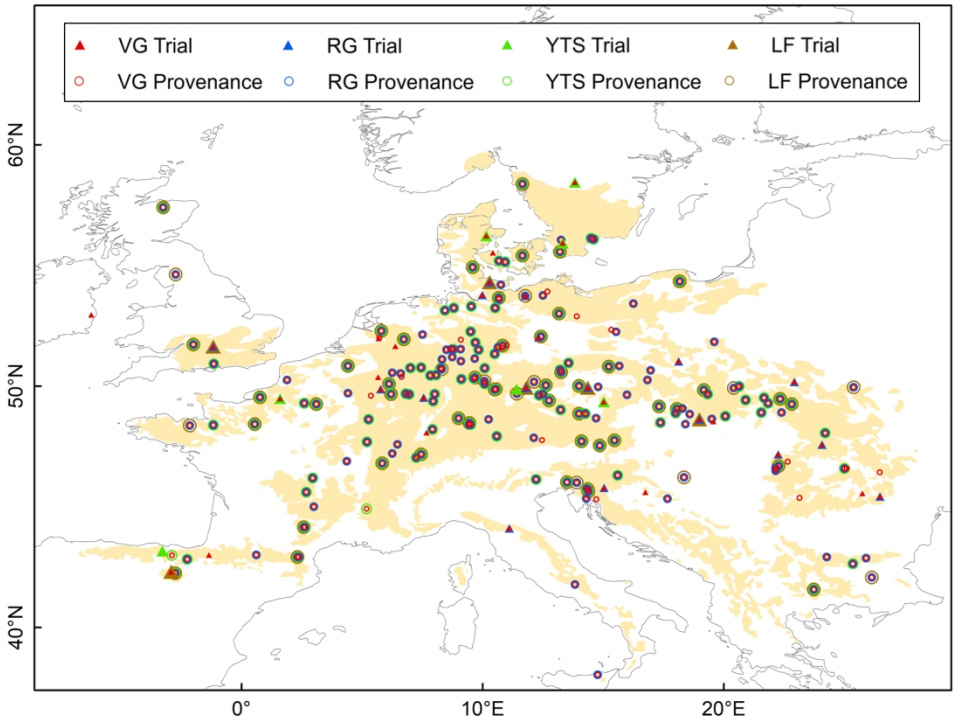

	VG	RG	YTS	LF	H-RG	H-LF
Measurements	203 105	34 237	41 309	7 863	34 237	12 087
Trees	108 415	31 339	37 433	7 863	31 339	10 634
Trials	36	19	7	7	19	6
Provenances	205	186	114	62	186	150
Age	2 to 15	8 to 15	2 to 6	12	8 to 15	6, 9, 11, 12, 15

Figure 1. Map: Distribution range of Fagus sylvatica L. (shaded in beige) and location of the provenances and trials by trait. Circles indicate the location of the provenances and triangles that of the trials. Different colors have been employed to indicate the different traits (VG: vertical growth; RG: radial growth; YTS: young tree survival; LF: leaf flushing). Table: The extent of data from the BeechCOSTe52 database (Robson et al. 2018) used for modelling. Measurements: total number of measurements; Trees: total number of individual trees; Trials: total number of trials; Provenances: total number of provenances, Age: the age at which the trees were measured. Columns indicate sample sizes for the traits used in the one-trait models and in the two-trait models.

160x160mm (300 x 300 DPI)

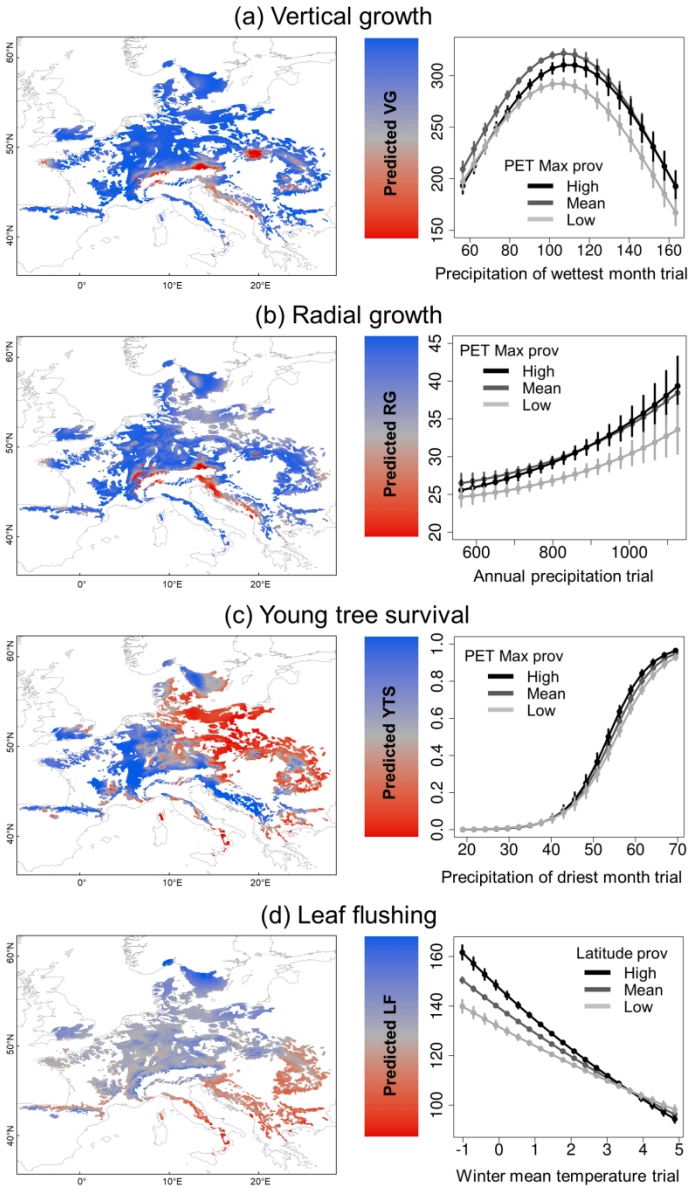

Figure 2. Spatial projections for (a) vertical growth (cm), (b) radial growth (mm), (c) young tree survival (probability) and (d) leaf flushing (Julian days) generated using one-trait models (maps on the left), and corresponding graphs of interactions between the best environmental predictor variable across the trials divided according to environment at the provenance for each of the four traits (graphs on the right). Interactions represent the differences in trait values that can be attributed to the provenance (interpretable as local adaptation driven by PET max in (a), (b), and (c) and driven by the latitude in (d)). Interactions also represent the differences in trait values that can be attributed to the environmental conditions of trial (interpretable as phenotypic plasticity driven by the environmental variables shown in the x-axis). Black, dark grey, and light grey lines represent high, medium and low values of the climatic variable of the provenances (as opposed to those of the trial, indicated on the x-axis). The vertical lines represent the confidence intervals. The maps display the trait projection for contemporary climate (inferred from 2000-2014 meteorological data) across the current species range. The color gradient depicts the clinal variation from low (red) to high (blue) values of each trait. The values of the different traits are represented in the following way: vertical growth (cm), radial growth (mm), probability of young tree survival (0 =dead,

1=alive) and leaf flushing (Julian days). PET max prov: maximal monthly potential evapotranspiration at the provenance; Latitude prov: latitude of the provenance.

135x230mm (300 x 300 DPI)

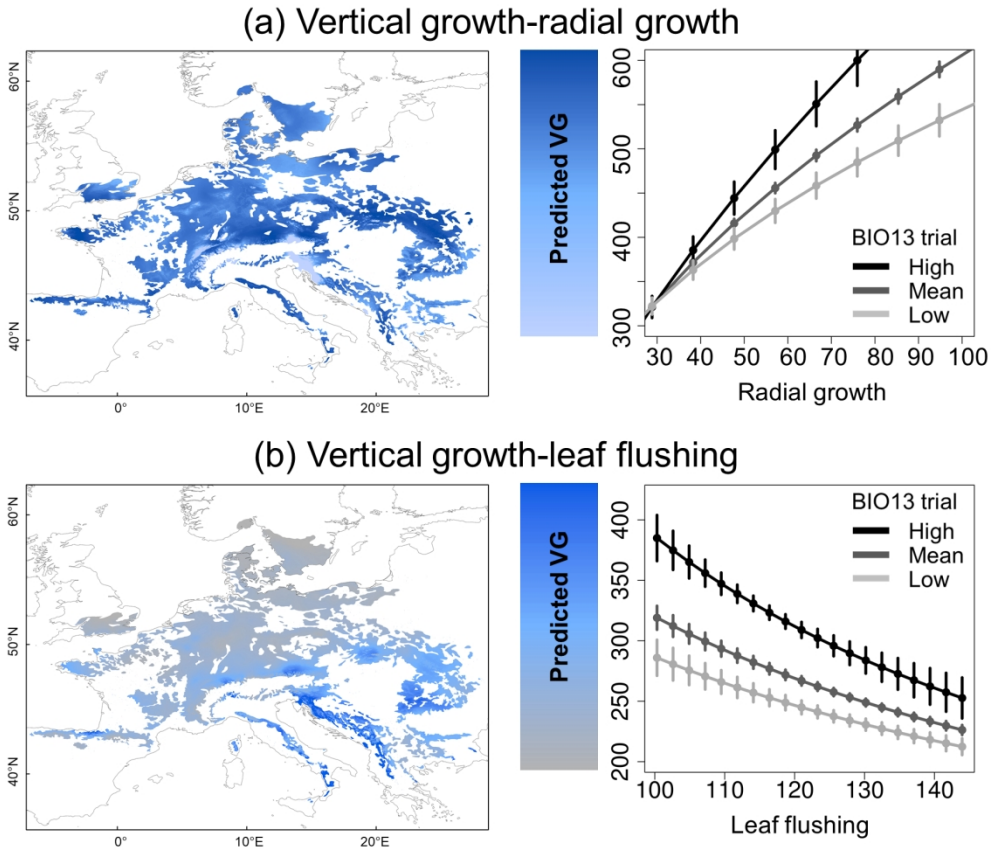

Figure 3. Spatial projections of vertical growth (cm) for (a) Vertical-radial growth model and (b) vertical growth-leaf flushing models (maps on the left), and the corresponding graphs of co-variation between vertical growth and the covariate: (a) DBH (mm) and (b) leaf flushing (Julian days). Black, dark grey, and light grey lines represent high, medium and low values of the precipitation of the wettest month of the trial (BIO13). The vertical lines represent the confidence intervals. The maps display the trait projection for contemporary climate (inferred from 2000-2014 meteorological data) across the current species range. The color gradient depicts the clinal variation in vertical growth from 200 cm (gray) to 600 cm (blue).

160x137mm (300 x 300 DPI)

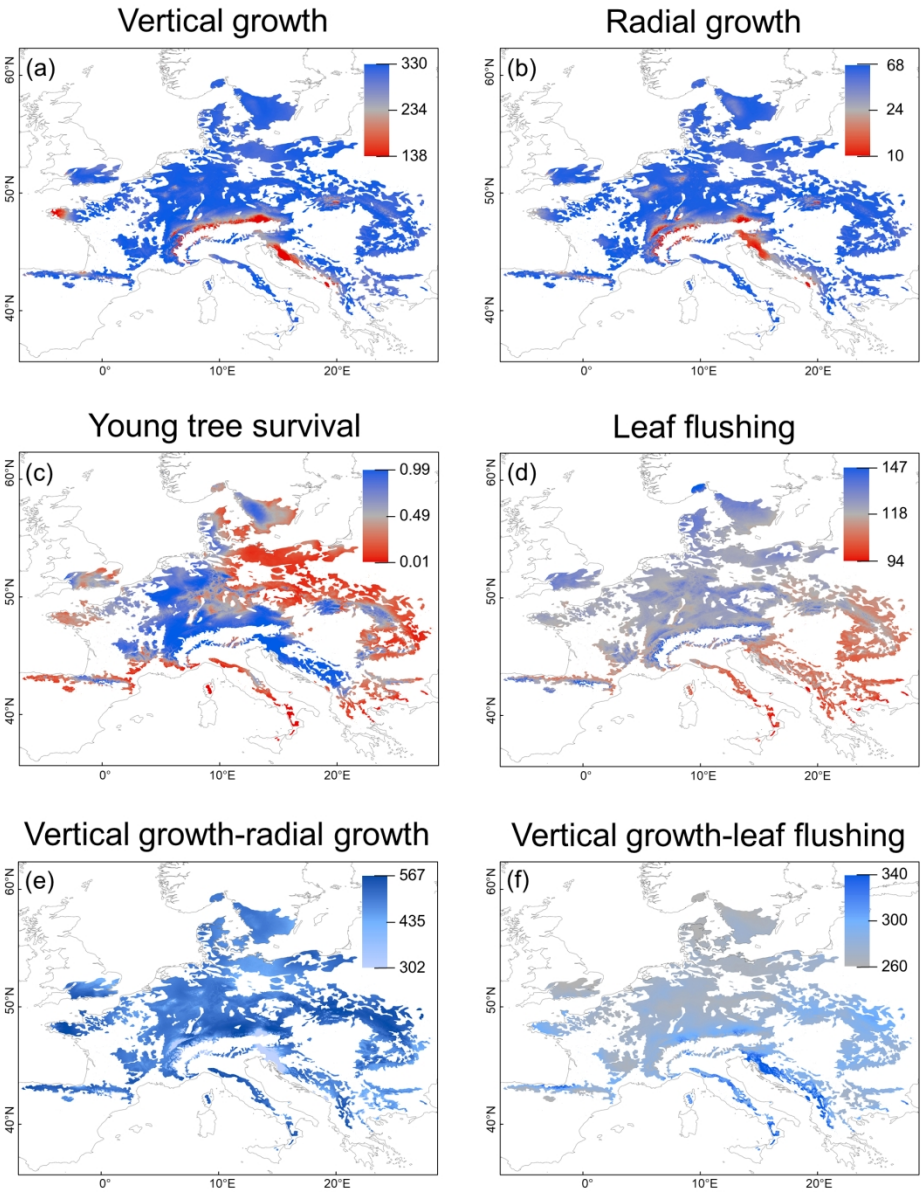

Figure 4. Spatial predictions for 2070 (RCP 8.5) across the species range for one-trait models: (a) vertical growth (cm); (b) radial growth (mm); (c) probability of young tree survival (0=dead; 1=alive); (d) leaf flushing (Julian days); and for two-trait models: (e) vertical growth (cm; co-variate radial growth) and (f) vertical growth (cm; co-variate leaf flushing). The color gradients depict the clinal variation from low (red) to high (blue) values.

165x209mm (300 x 300 DPI)

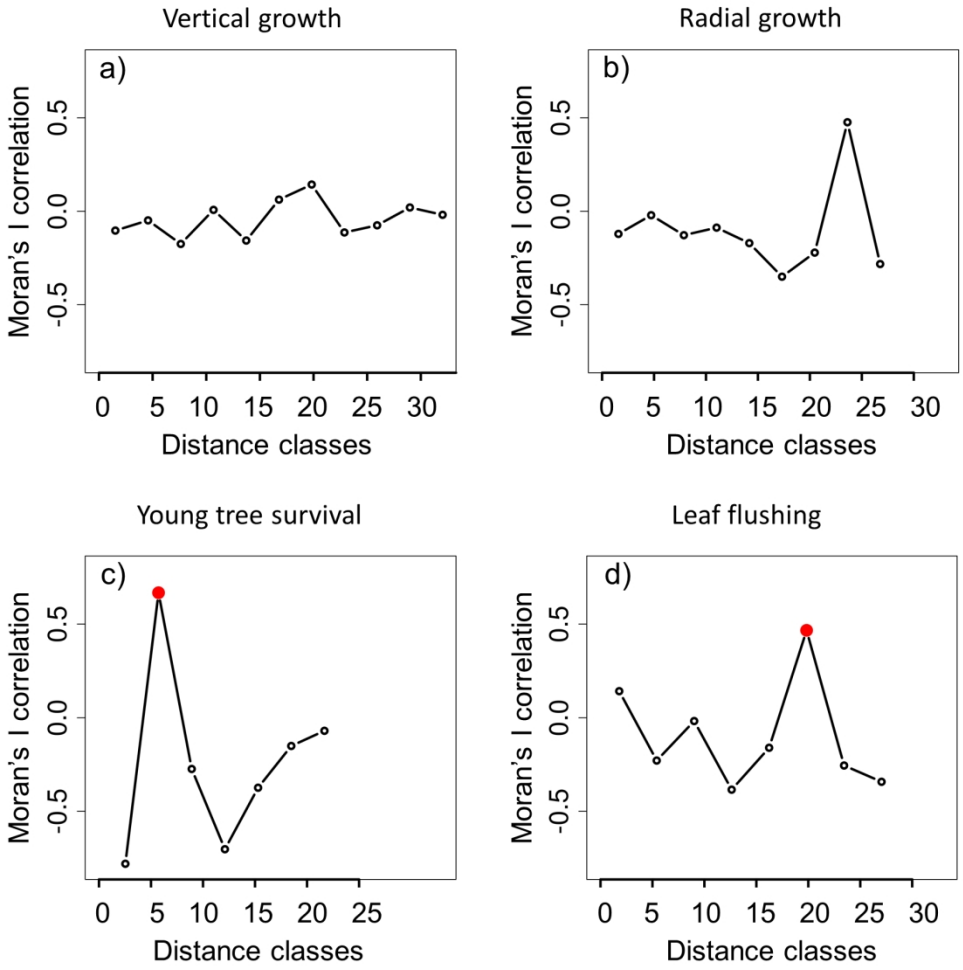

Supporting Information Figure S1.1. Correlograms of Moran's I correlation coefficient (y-axis) and the distance classes (x-axis) for vertical (a) and radial (b) growth, young tree survival (c), and leaf flushing (d). Moran's correlation coefficient ranges between 1 and -1. Distance classes are Euclidian and in degrees. Distances of significant spatial dependence are shown in red (significant values $p < 0.05$).

160x157mm (300 x 300 DPI)

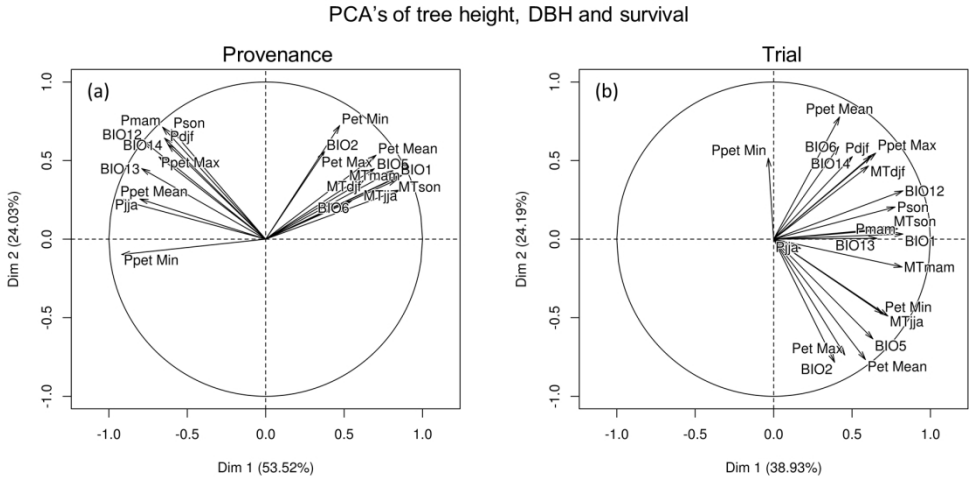

Supporting Information Figure S1.2. Results of PCA for checking for co-linearity and reducing the climatic space to select the final climate variables for the stepwise procedure used in the models on traits vertical and radial growth, and young tree survival, conducted by provenance (a) and by trial (b). When two variables are strongly correlated, only one of them was used in models. The variance explained by the first two axes is indicated in the figures.

160x80mm (300 x 300 DPI)

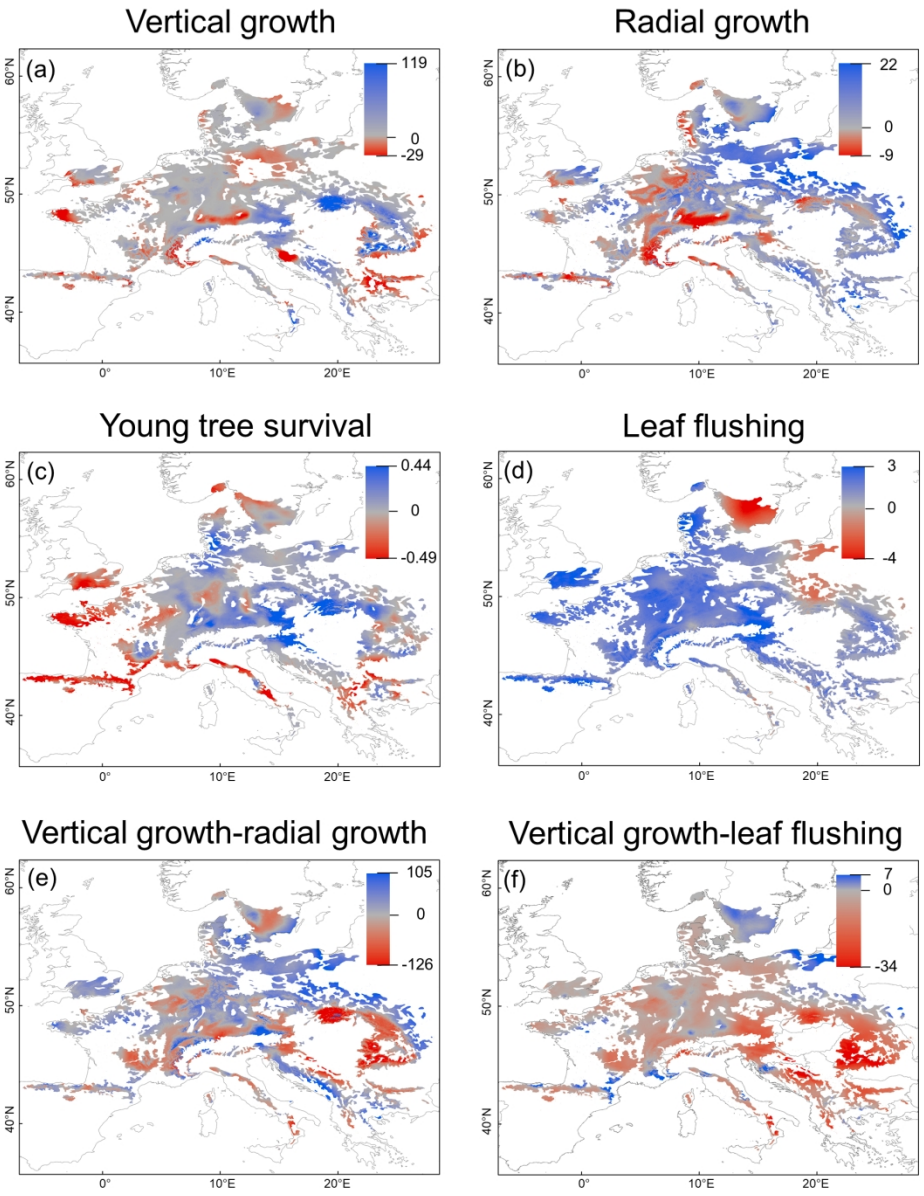

Supporting Information Figure S1.3. Differences in predictions between future (2070) and contemporary (2000-2014) climate for one-trait models in beech range: (a) vertical growth of 12 year-old trees (in cm); (b) radial growth of 12 year-old trees (in mm); (c) probability of young tree survival of 6 year-old trees; (d) leaf flushing of 12 year-old trees (difference in Julian days); and for two-trait models: (e) vertical growth (in cm; co-variate radial growth) and (f) vertical growth (in cm; co-variate leaf flushing). The color gradient depicts the clinal variation from low (red) to high (blue) values.

165x209mm (300 x 300 DPI)